Central nervous system (CNS)–resident natural killer cells suppress Th17 responses and CNS autoimmune pathology

Junwei Hao,[1,2,3] Ruolan Liu,[2] Wenhua Piao,[2] Qinghua Zhou,[1] Timothy L. Vollmer,[4] Denise I. Campagnolo,[2] Rong Xiang,[3] Antonio La Cava,[5] Luc Van Kaer,[6] and Fu-Dong Shi[1,2]

[1]Department of Neurology, Tianjin Neurological Institute, Tianjin Medical University General Hospital, Tianjin 300052, China
[2]Department of Neurology, Barrow Neurological Institute, St. Joseph's Hospital and Medical Center, Phoenix, AZ 85013
[3]School of Medicine, Nankai University, Tianjin 300071, China
[4]Department of Neurology, University of Colorado Denver School of Medicine, Aurora, CO 80045
[5]Department of Medicine, University of California, Los Angeles, Los Angeles, CA 90095
[6]Department of Microbiology and Immunology, Vanderbilt University School of Medicine, Nashville, TN 37232

Natural killer (NK) cells of the innate immune system can profoundly impact the development of adaptive immune responses. Inflammatory and autoimmune responses in anatomical locations such as the central nervous system (CNS) differ substantially from those found in peripheral organs. We show in a mouse model of multiple sclerosis that NK cell enrichment results in disease amelioration, whereas selective blockade of NK cell homing to the CNS results in disease exacerbation. Importantly, the effects of NK cells on CNS pathology were dependent on the activity of CNS-resident, but not peripheral, NK cells. This activity of CNS-resident NK cells involved interactions with microglia and suppression of myelin-reactive Th17 cells. Our studies suggest an organ-specific activity of NK cells on the magnitude of CNS inflammation, providing potential new targets for therapeutic intervention.

CORRESPONDENCE
Fu-Dong Shi:
fshi@chw.edu

Abbreviations used: CNS, central nervous system; DHE, dihydroethidium; EAE, experimental autoimmune encephalomyelitis; mDC, myeloid DC; MOG, myelin oligodendrocyte glycoprotein; MS, multiple sclerosis; pDC, plasmacytoid DC; ROS, reactive oxygen species.

Inflammatory and immune responses within the central nervous system (CNS) significantly affect the clinical presentation and outcome of brain disorders, including stroke, trauma, Alzheimer's disease, Parkinson's disease, epilepsy, encephalomyelitis, and multiple sclerosis (MS; Weiner and Selkoe, 2002). In the case of MS and its animal model experimental autoimmune encephalomyelitis (EAE), a classical inflammatory disease characterized by cellular influx, demyelination, and axonal damage of the CNS, initiation of disease is controlled by an interplay between cells of the innate and adaptive immune systems (Steinman, 1996; Wekerle, 1998). NK cells are an important cell subset of the innate immune system represented by large granular lymphocytes that respond rapidly to a variety of insults with cytolytic activity and cytokine secretion (Kärre et al., 1986; Biron et al., 1999; Yokoyama and Plougastel, 2003; Raulet, 2004; Lanier, 2008). Recently, there has been a growing understanding of NK cells, particularly with regard to their roles in autoimmunity in the joints, pancreas, and CNS (French and Yokoyama, 2004; Shi and Van Kaer, 2006; Wu et al., 2007; Feuerer et al., 2009). Mechanisms by which NK cells could have an impact on autoimmune responses include a rapid cytokine release by NK cells before autoreactive helper T cell differentiation and modulation of interactions between autoreactive T cells, B cells, and APCs (Chambers et al., 1996; Shi et al., 2000; Martín-Fontecha et al., 2004; Laouar et al., 2005). However, much of this evidence is derived from studying peripheral lymphoid organs. Whether NK cells can act in target organs of autoimmunity such as the CNS has not yet been investigated.

The manifestations of CNS disease, such as MS and EAE, require the homing of myelin-reactive T cells to the CNS, where T cells undergo reactivation, further differentiation, and expansion. The spectrum of APCs, antigens,

J. Hao, R. Liu, and W. Piao contributed equally to this paper.

The Rockefeller University Press $30.00
J. Exp. Med. Vol. 207 No. 9 1907-1921
www.jem.org/cgi/doi/10.1084/jem.20092749

The Journal of Experimental Medicine

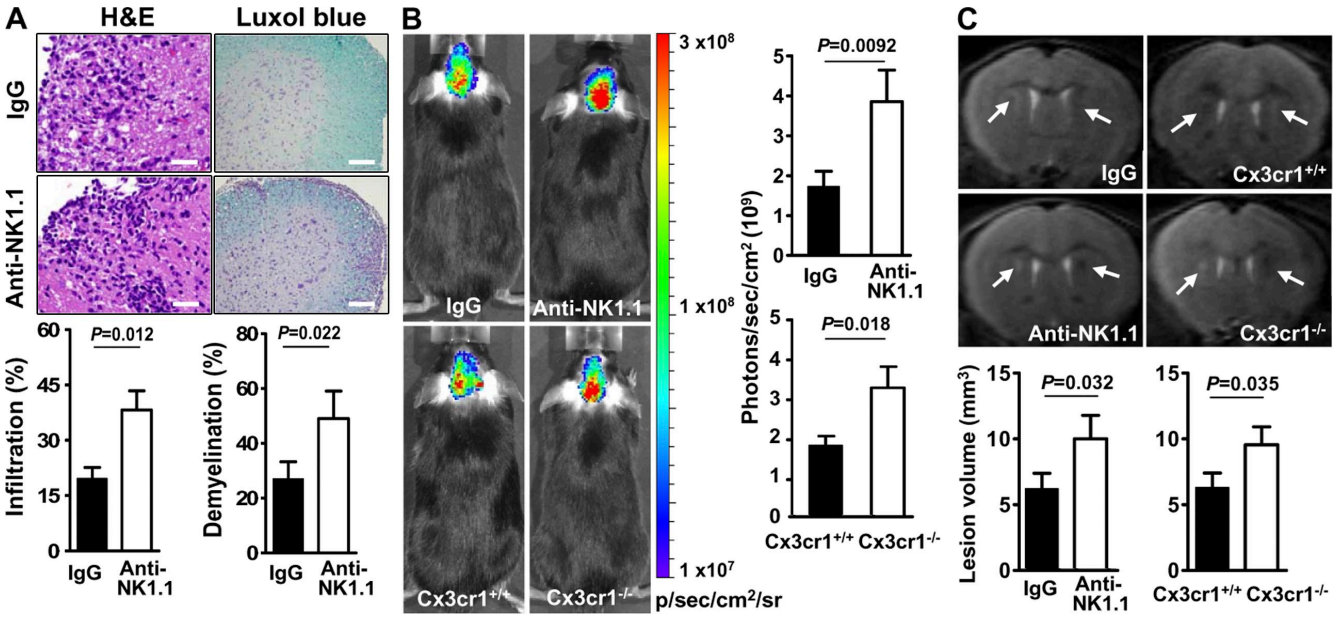

Figure 1. NK cells control the magnitude of CNS inflammation. (A) Microscopy of CNS sections from MOG-immunized mice that received control IgG or anti-NK1.1 mAb. H&E (left) and luxol fast blue (right) staining reveals the intensity of cell infiltration and myelin integrity, respectively. Graphs show quantified data. Bars, 100 µm. (B) Visualization and quantification of brain inflammation by in vivo bioluminescence imaging. Graphs show quantified data. (C) T2-weighted periventricular images were obtained with a 7T MR scanner. Arrows indicate focal lesions located around the lateral ventricle and increased signal intensity on T2-weighted lesions. Pathology and imaging experiments were conducted in groups of mice (n = 4–8) between 15 and 20 d after immunization. P-values were determined by a Student's t test. Data are representative of two independent experiments (mean ± SEM).

and neuroimmune interactions within the CNS are unique (Shi and Ransohoff, 2010), and the outcome of an immune response cannot be predicted solely by the events that occurred in the periphery. NK cells readily home to the CNS under an array of pathological circumstances (Shi and Ransohoff, 2010). It is not known whether these NK cells are simply passive migrants or actively participate in the CNS pathogenesis.

In this paper, we investigated the role of NK cells in the CNS in shaping autoimmunity and pathology. Our findings have revealed a critical role of CNS-resident NK cells in controlling the magnitude of CNS inflammation. This observation could be exploited for therapeutic intervention in CNS disease.

RESULTS

Peripheral versus CNS-resident NK cells in shaping CNS inflammation and pathology

Studies of NK cell function in vivo have often been challenging because of the unavailability of mice that selectively lack NK cells (Yokoyama and Plougastel, 2003; Shi and Van Kaer, 2006). To overcome this limitation, we have combined several approaches, including NK cell–depleting mAb, interruption of NK cell homing, and NK cell enrichment (Fig. S1).

To dissect the role of NK cells in the development of inflammatory and autoimmune responses in the CNS, we immunized C57BL/6 (B6) mice with myelin oligodendrocyte glycoprotein (MOG) peptide, which produces a monophasic neurological deficit resembling a form of human MS known as acute disseminated encephalomyelitis. Previously, it was demonstrated that depletion of NK1.1$^+$ cells by anti-NK1.1 mAb (clone PK136) dramatically enhanced EAE severity (Zhang et al., 1997; Xu et al., 2005). We confirmed these findings and verified that disease exacerbation was caused by the removal of NK cells rather than NKT cells (Fig. S2). Pathologically, the mice treated with anti-NK1.1 mAb exhibited pronounced cellular infiltrates, inflammation, and demyelination, as indicated by immunohistochemical staining, bioluminescence imaging, and high-field MRI, respectively (Fig. 1, A–C).

We considered two possibilities for the exaggerated CNS disease observed in MOG-immunized mice systemically depleted of NK cells: (1) enhanced pathogenic T cell infiltration from the periphery to the CNS, or (2) attenuated suppressive effects of NK cells on pathogenic T cells within the CNS. To distinguish between these two possibilities, we used a model of selective NK cell deficiency in the CNS. We used mice in which the chemokine receptor Cx3cr1 gene was replaced with a cDNA encoding GFP (Jung et al., 2000). We previously demonstrated that CX3CR1 is responsible for recruiting NK cells to the inflamed CNS in mice with EAE (Huang et al., 2006) and that Cx3cr1$^{GFP/GFP}$ (Cx3cr1$^{-/-}$) mice exhibit a selective deficit in NK cell homing to the CNS, whereas NK cells in other organs are not affected (Huang et al., 2006). Pathologically, the MOG-primed Cx3cr1$^{-/-}$ mice had frequent hemorrhagic brain and spinal cord lesions (Huang et al., 2006). Increased inflammation and disease activity were further illustrated by neuroimaging (Fig.1, B and C).

Collectively, these results suggest that NK cell depletion from all organ systems augments the magnitude of CNS inflammation and pathology. The finding that Cx3cr1$^{-/-}$ mice with reduced

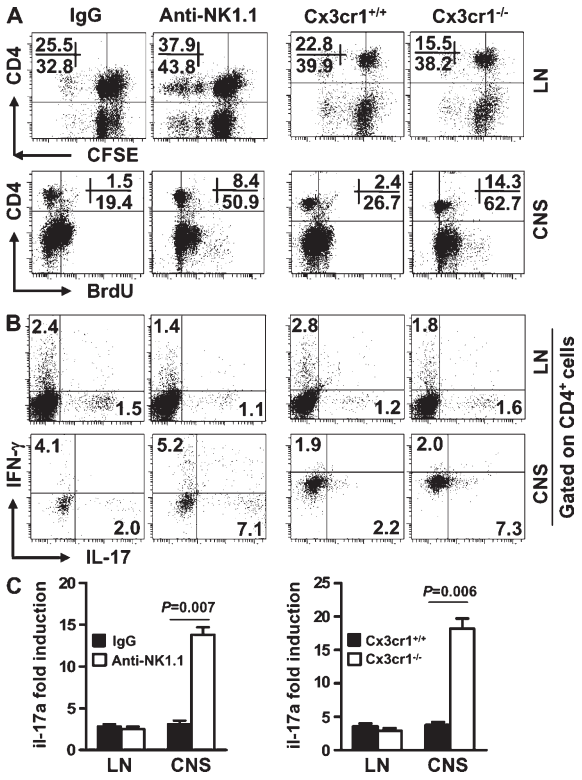

Figure 2. Influence of NK cell depletion or impaired homing of NK cells to the CNS on myelin-reactive Th1 and Th17 cell responses in the periphery and the CNS. Groups of mice (receiving mouse IgG or anti-NK1.1 mAb, and Cx3cr1$^{+/+}$ or Cx3cr1$^{-/-}$) were immunized with MOG/CFA/PT and sacrificed between days 12 and 20 after immunization. Lymph node (LN), spleen, and CNS cells were isolated. (A) Expansion of CD4$^+$ T cells from lymphoid organs or CNS was assessed by CFSE dilution or BrdU incorporation assay, respectively. (B) Lymphoid or CNS cells were restimulated with MOG overnight, and IFN-γ– and IL-17–expressing CD4$^+$ T cells were measured by intracellular staining. (C) Il-17a mRNA of sorted CD4$^+$ T cells was measured by qRT-PCR. Data are representative of four independent experiments (n = 18–25/group). Error bars represent the means ± SEM. P = 0.007 and 0.006 for IL-17–expressing CD4$^+$ cells (Student's t test).

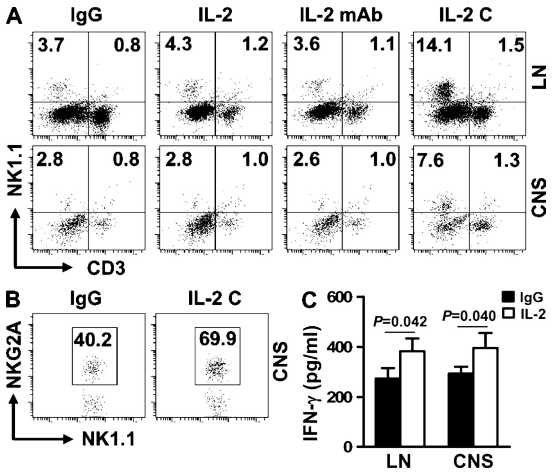

Figure 3. Frequencies and phenotype of NK cells in MOG-immunized mice treated with IL-2 complexes. Upon EAE induction with MOG, B6 mice were treated with control IgG, IL-2, anti–IL-2 mAb (S4B6), or a combination of IL-2 and anti–IL-2 mAb (IL-2 C) i.p. as indicated in Materials and methods. Single cell suspensions were prepared from the spleen and CNS of mice on days 12–20, and the frequencies and phenotypes of mononuclear cells were analyzed by FACS. (A) The frequencies of NK and NKT cells in the periphery and CNS. (B) Expression of NKG2A on NK cells. (C) Production of IFN-γ by NK cells. P-values were determined by a Student's t test. The dot plots are representative of three separate experiments (n = 5–15/group). Error bars represent the means ± SEM.

CNS-infiltrating NK cells but intact peripheral NK cells exhibited similar clinical and pathological features to NK cell–depleted animals suggests that CNS NK cells are crucial in this process.

Suppression of myelin-reactive Th17 cells by NK cells is restricted to the CNS

Autoreactive T cells, particularly the CD4$^+$ subset, home to the CNS, reencounter myelin antigens in this location and undergo reactivation and further expansion. This process is believed to be a prerequisite step for the expression of disease in EAE and perhaps in MS. Therefore, we investigated how NK cell depletion, or failure to home to the CNS, might influence the capacity of CD4$^+$ T cells to proliferate and further differentiate into Th1 or Th17 cells. Lymph node (or splenic) CD4$^+$ T cells from mice treated with anti-NK1.1 mAb divided 1.5-fold more frequently than CD4$^+$ T cells from control mice (Fig. 2 A and not depicted). CD4$^+$ T cells from CNS isolates divided four- to sixfold more frequently in NK cell–depleted mice than in control mice (Fig. 2 A). As expected, lymph node CD4$^+$ T cells from Cx3cr1$^{-/-}$ mice proliferated at a similar magnitude as those from WT mice, whereas CNS-derived Cx3cr1$^{-/-}$ CD4$^+$ T cells proliferated more vigorously (Fig. 2 A). These results indicate that NK cells suppress CD4$^+$ T cell proliferation and this suppression is more pronounced in the CNS than in peripheral organs.

Next, we assessed the impact of NK cell depletion or their failure to home to the CNS on the phenotype of CD4$^+$ T cells. Depletion of NK cells reduced MOG-reactive IFN-γ–producing Th1 cell responses in lymph node but not the CNS (Fig. 2 B). In contrast, MOG-reactive CD4$^+$ Th17 cell responses were increased three- to fivefold in the CNS of NK cell–depleted mice. Importantly, the enhancement of Th17 cell responses was almost exclusive to CD4$^+$ T cells in the CNS (Fig. 2 B). Quantitative (q) RT-PCR for il-17a transcripts using sorted CD4$^+$ T cells confirmed this finding (Fig. 2 C). These results of NK cell depletion were mirrored by an increase of Th17 phenotype cells in Cx3cr1$^{-/-}$ mice (Fig. 2, B and C). The global levels of IL-17 and IFN-γ quantified using lymph node, brain, and spinal cord homogenates were consistent with those observed for CD4$^+$ T cells (Fig. S3). Depletion of NK cells also led to enhanced proliferation of CD8$^+$ T cells in lymph nodes, but such effects were absent in the CNS (Fig. S4, A and B). In addition, the frequency of IL-17$^+$ CD8$^+$ T cells was minimal and did not change significantly upon NK cell depletion (Fig. S4 C). Thus, suppression of myelin-reactive CD4$^+$ Th17 cells by NK cells is largely restricted to the CNS compartment.

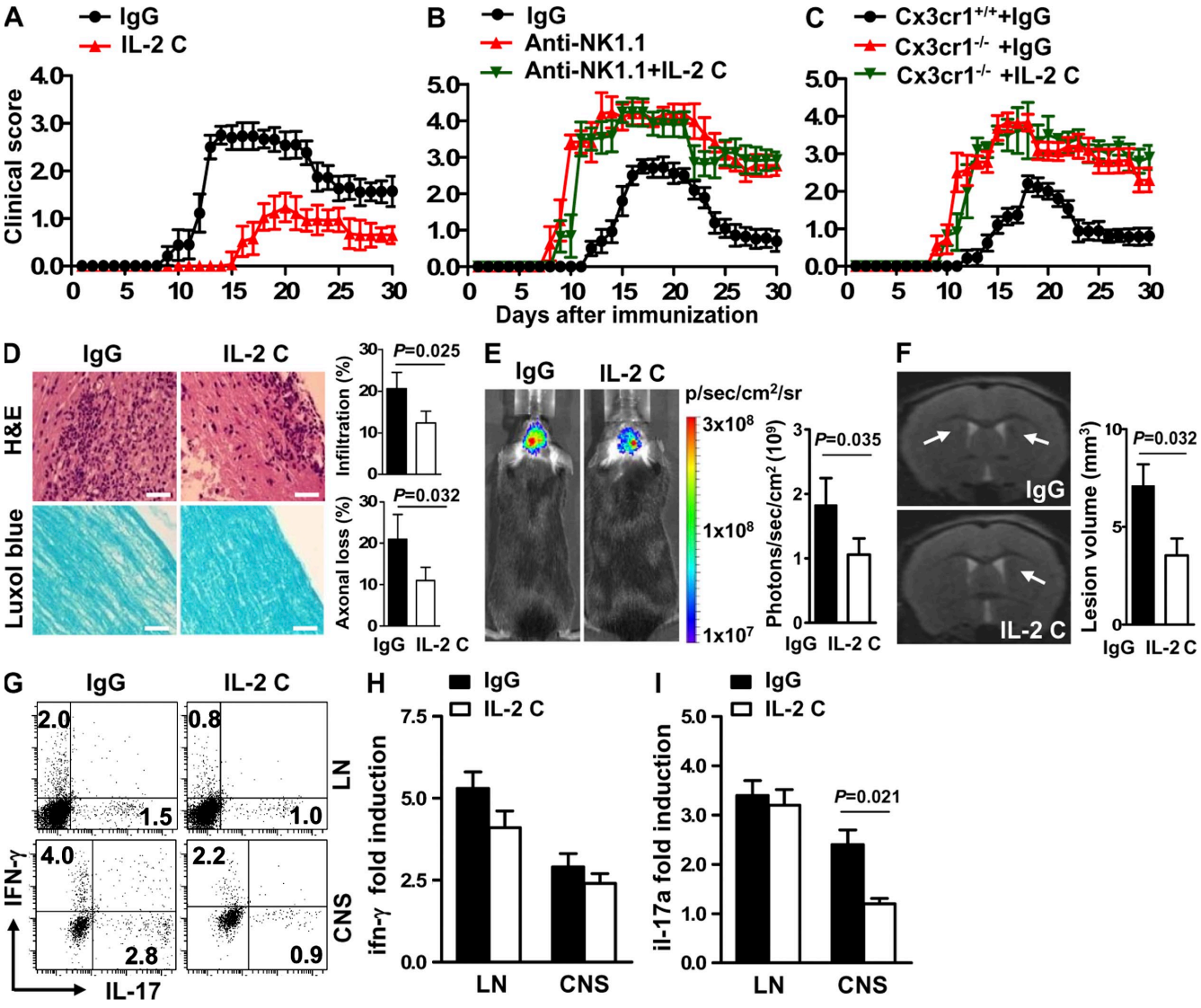

Figure 4. IL-2 complexes attenuate EAE and silence Th17 cell responses in the CNS. (A) Effect of IL-2 complexes on the development and progression of EAE. n = 12–16/group. Data are pooled from three independent experiments. $P < 0.01$ between days 9 and 21 and $P < 0.05$ between days 22 and 30 (Mann-Whitney U test). (B and C) Effects of IL-2 complexes on the development and progression of EAE in mice that received anti-NK1.1 mAb (B; n = 8/group) or in Cx3cr1$^{-/-}$ mice (C; n = 8–12/group). Data are pooled from two independent experiments. Error bars represent the means ± SEM. $P > 0.05$ for any time point (Mann-Whitney U test). (D) Cellular infiltration (top) and demyelination (bottom) were analyzed using CNS sections harvested from days 12–20 after immunization. Bars, 100 µm. (E) Visualization and quantification of brain inflammation by in vivo bioluminescence imaging at day 15 after immunization. (F) In vivo MRI brain images of mice treated with IgG or IL-2 complexes (IL-2 C) showed a decrease in inflammation and demyelination in IL-2 complex–treated mice. Focal lesions (arrows) were located around the lateral ventricle in IgG-treated mice and increased signal intensity on T2-weighted lesions, which were attenuated in IL-2 complex–treated mice. Data from D–F are representative of two independent experiments (n = 4–6/group). Error bars represent the means ± SEM. P-values were determined by a Student's t test. (G) Lymphoid or CNS cells were restimulated with MOG overnight, and IFN-γ– and IL-17–expressing CD4$^+$ T cells were measured by intracellular staining. (H and I) qRT-PCR of IFN-γ and IL-17 transcripts from sorted CD4$^+$ T cells. Data from G–I are representative of four independent experiments (n = 6–12/group). Error bars represent the means ± SEM. P-values were determined by a Student's t test.

IL-2–mAb complexes expand NK cells with a unique phenotype

Our data using NK cell–depleting antibodies and Cx3cr1$^{-/-}$ mice show the inhibitory function of NK cells against autoimmune responses within the CNS. An alternative approach to investigate the role of NK cells in this process is to enrich these cells in vivo. Prior studies have shown that anti–IL-2 mAbs (clone S4B6) guide IL-2 toward cells with intermediate-affinity IL-2 receptors and stimulate the proliferation of memory phenotype CD8$^+$ T cells and NK cells (Boyman et al., 2006). We coupled IL-2 with IL-2 mAb (referred to as IL-2 complexes or IL-2 C hereafter) and examined the effects on NK cells and other lymphocytes during EAE. During our initial experiments, we developed an injection regimen of frequency and dosage that conferred maximal expansion and

maintenance of NK cells, with its associated disease protection (Table S1 and not depicted). Using this protocol, we showed that IL-2 complexes were more efficient than IL-2 or anti–IL-2 mAb alone in expanding NK cells, both in the lymph nodes and the CNS (Fig. 3 A). With regard to their phenotypic characteristics, NK cells from IL-2 complex–treated mice exhibited no dramatic alterations in the expression of NKG2D, Ly49D, CD244 (2B4), Ly49A, and Ly49C (not depicted), a significant up-regulation of the inhibitory receptor NKG2A on NK cells in the CNS (Fig. 3 B), and an intact capacity to produce IFN-γ (Fig. 3 C). IL-2 complexes also increased the numbers of $CD8^+$ T cells with a predominantly memory phenotype and a concurrent decrease in $CD4^+$ T cells. $CD4^+CD25^+$ T cells and NKT cells were also increased at varying degrees (Fig. S5).

CNS-resident NK cells inhibit EAE in the presence of IL-2 complexes

We evaluated the impact of IL-2 complexes on the clinical course of EAE. Compared with control mice, the onset of EAE in treated mice was delayed and neurological deficits were relatively mild (Fig. 4 A). Accordingly, these mice also exhibited attenuated cellular infiltrates and demyelination (Fig. 4, D–F). While assessing the influence of IL-2 complexes on MOG-reactive Th cell responses, we found that IL-17 mRNA expression and protein production by lymph node cells were not significantly altered by IL-2 complexes, whereas IL-17 production by $CD4^+$ T cells in the CNS was dramatically reduced (Fig. 4, G–I). IFN-γ–producing $CD4^+$ T cells within the CNS were also reduced (Fig. 4 G). Alterations for $CD8^+$ T cell–derived IFN-γ and IL-17 were minimal (Fig. S4).

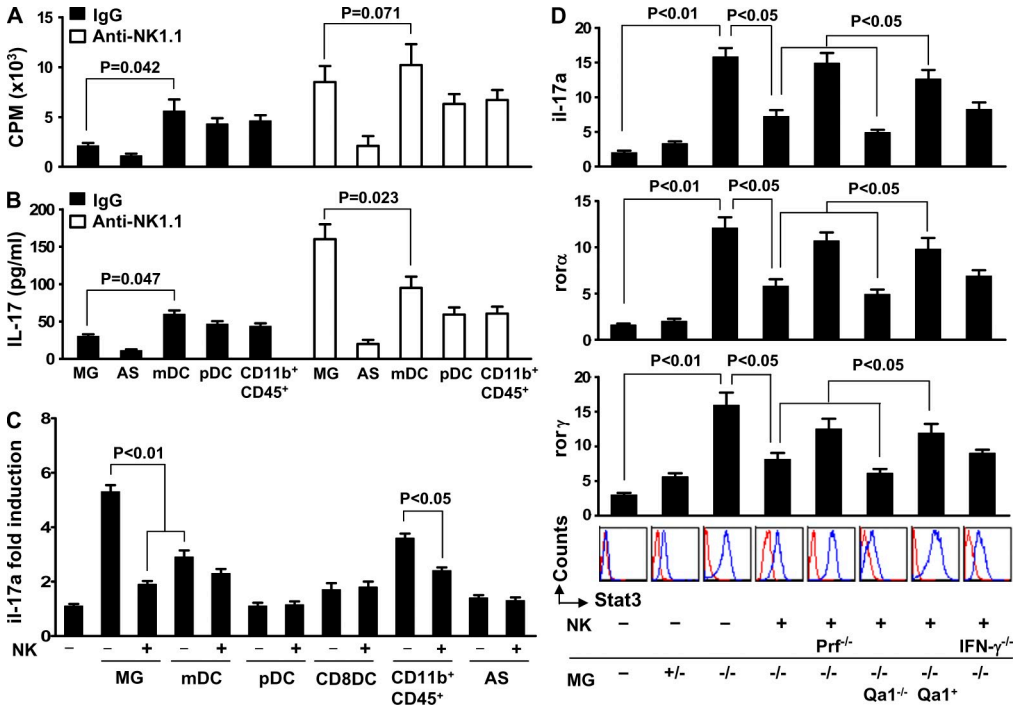

Figure 5. Effects of NK cells on the capacity of microglia and other CNS-derived APCs to promote myelin-reactive T cell proliferation and Th17 responses. (A) Proliferation of naive $CD62L^{high}$ MOG_{35-55}-specific $CD4^+$ transgenic 2D2 T cells cultured with microglia, astrocytes (AS), mDCs, pDCs, $CD11b^+CD45^+$, or irradiated $CD4^-$ splenocytes from MOG-primed mice at the peak of EAE disease at an APC/T cell ratio of 5:1, in the presence or absence of 10 µg/ml MOG_{35-55} peptide. Mice were treated with control IgG or anti-NK1.1 before immunization. Results are expressed as the changes in counts per minute (CPM). Irradiated $CD4^-$ splenocytes stimulate 2D2 cells at 2/3 of the capacity of mDCs. (B) Release of IL-17 by T helper cell supernatant from A after 72 h. (C) Capacity of CNS-derived APCs to drive Th17 cell responses and to be affected by NK cells. Naive ($CD25^-CD62L^{high}CD44^{low}$) $CD4^+$ T cells were sorted from lymph nodes and spleens of 2D2 transgenic mice. Subsequently, 2×10^5 cells of the indicated APC types and NK cells (all isolated from the CNS) were added to the culture. NK cells from the IL-2 complex–treated mice were injected into the brain. Il-17a transcripts were quantified by qRT-PCR. Data in A–C are representative of two independent experiments using cells from 15–20 mice/group. MG, microglia. Error bars represent the means ± SEM. P-values were determined by an ANOVA test. (D) Interactions between NK cells and microglia influence myelin-reactive Th17 cells in vivo and the importance of the NKG2A–Qa1 pathway. Naive ($CD25^-CD62L^{high}CD44^{low}$) $CD4^+$ T cells were sorted from lymph nodes and spleens of 2D2 mice. Subsequently, 2×10^5 cells were injected i.v. into MOG/CFA/PT-primed $RAG1^{-/-}\gamma c^{-/-}$ mice. Simultaneously, the same numbers of microglia from $Cx3cr1^{+/-}$ ($MG^{+/-}$) and $Cx3cr1^{-/-}$ ($MG^{-/-}$) mice and NK cells from the IL-2 complex–treated mice were injected into the brain as previously described (Cardona et al., 2006b). STAT3 phosphorylation was quantified by FACS and compared in mice receiving $CD4^+$ T cells alone or mice that also received microglia from $Cx3cr1^{+/-}$ or $Cx3cr1^{-/-}$ mice. RNA was isolated from 2D2 $CD4^+$ cells and Rorα, Rorγ (also know as Rorc), and Il-17a transcripts were quantified by qRT-PCR. Data represent three experiments with 15–22 mice per group each. Error bars represent the means ± SEM. P-values wre determined by an ANOVA test. For C and D, + and − denote culture with or without NK cells.

To assess whether NK cells mediated the protection against EAE during IL-2 complex therapy, we depleted NK cells before EAE induction and IL-2 complex treatment. Removal of NK cells almost completely abolished the therapeutic effects of IL-2 complexes (Fig. 4 B). Because anti-NK1.1 mAbs remove NK cells from both periphery and CNS, we asked whether NK cells in the periphery, the CNS, or both contributed to the protective effects of IL-2 complexes on EAE. For this purpose, we treated Cx3cr1$^{-/-}$ mice with IL-2 complexes upon EAE induction. The clinical features of EAE were nearly identical in Cx3cr1$^{-/-}$ mice that received control IgG or IL-2 complexes (Fig. 4 C). Injection of anti-NK1.1 mAb into the brain eliminated NK cells from the CNS without altering peripheral NK cells and largely abrogated the therapeutic effect of IL-2 complexes (unpublished data). Thus, we conclude that the effects of IL-2 complexes on EAE depend on CNS-resident NK cells.

In dissecting potential contributions of other IL-2R–bearing cells, we treated CD1d$^{-/-}$ mice (Mendiratta et al., 1997; devoid of NKT cells), CD8$^{-/-}$ mice, and mice depleted of CD25^{+} cells with IL-2 complexes before EAE induction. IL-2 complex injection attenuated EAE in CD1d$^{-/-}$ mice and mice depleted of CD25^{+} cells (Fig. S6, A and B). The magnitude of the disease attenuation in these mice was similar to that observed in WT B6 mice (Fig. 4 A). IL-2 complexes partially lost their effectiveness against EAE in CD8$^{-/-}$ mice (Fig. S6 C). Furthermore, unlike NK cells (see Fig. 6 A) CD8^{+} T cells did not reside in close proximity with microglia. CD8^{+} T cells were capable of killing microglia, albeit much less effectively than NK cells (unpublished data). Collectively, these data indicated that NKT cells, T reg cells, and CD8^{+} T cells do not contribute in a significant manner to the EAE phenotype in mice receiving IL-2 complexes.

NK cells condition the cytokine microenvironment in the CNS

Our finding that modulation of NK cells affects myelin-reactive Th17 cells in the CNS suggested that NK cells can influence the cytokine environment in a different manner in the CNS and in the periphery. To test this possibility, we compared the cytokine profile in these two anatomical compartments. Lymph node culture supernatants, brain, and spinal cord homogenates from MOG-immunized mice that received anti-NK1.1 mAb or from MOG-immunized Cx3cr1$^{-/-}$ mice had a tendency for an increased expression of the Th17-polarizing cytokines IL-1β, IL-6, TGF-β1, and TNF, as well as the pro-inflammatory chemokines MCP-1, MIP-1α, and MCP-1β, as compared with controls. We observed the opposite in mice treated with IL-2 complexes, and such alterations appeared to be milder in lymph nodes (Fig. S3).

NK cells suppress the induction of Th17 transcription factors by microglia

Our observation that NK cell–mediated inhibition of CNS inflammation and Th17 cell responses are restricted to the CNS suggested the involvement of additional players specific to the CNS. Previous studies have elegantly demonstrated that myeloid DCs (mDCs) presenting endogenous myelin peptides preferentially polarize CD4^{+} T cells toward the Th17 cell lineage in a relapsing remitting EAE model (Bailey et al., 2007). We therefore compared the capacity of microglia and several types of APCs from the CNS, either migrated to this location or resident in the CNS, in priming 2D2 MOG-specific T cells. In agreement with Bailey et al. (2007), mDCs were most potent among the CNS-derived APCs, including microglia, astrocytes, plasmacytoid DCs (pDCs), and CD11b^{+}CD45^{+} cells (microglia and macrophages), in inducing 2D2 T cell proliferation (Fig. 5 A) and production of IL-17 (Fig. 5 B) in mice with EAE. It is of note that when these APCs were isolated from MOG/CFA-primed mice that also received anti-NK1.1 mAb, their capacity to induce 2D2 cell proliferation and production of IL-17 was increased (Fig. 5, A and B). Interestingly, microglia emerged as the most potent APCs in driving Th17 cells, despite their capacity to induce 2D2 cell proliferation at levels comparable to those of mDCs (Fig. 5, A and B). Similar results were obtained using APCs from Cx3cr1$^{-/-}$ mice (in which homing of NK cells to the CNS is severely impaired; unpublished data).

Table I. Microglia are a major source of Th17-polarizing cytokines in the absence of NK cells

Cytokines	Cell source		
	Microglia	mDCs	Astrocytes
IL-1	283.5 ± 9.0**	151.4 ±19.8	40.0 ± 3.9
IL-6	478.3 ± 49.7*	139.1 ±16.3	48.0 ± 6.3
IL-23	233.5 ± 21.7**	91.7 ± 12.5	81.3 ± 12.5

Microglia, mDCs, and astrocytes were isolated from CNS tissues, and cytokine release was measured by ELISA. n = 4/group. Data represent three independent experiments. *, P < 0.05; **, P < 0.01, Student's t test.

Given that NK cells alter the cytokine microenvironment in the CNS (Fig. S3) and that the best defined factors that determine Th cell subset differentiation are cytokines and chemokines that are present at the initiation stage of T cell receptor ligation (O'Garra, 1998), we compared the capacity of the CNS-derived APC to release Th17 cell–polarizing cytokines and determined whether this process could be altered by NK cells. Similar amounts of IL-1, IL-6, and IL-23 were produced by microglia and mDCs from control mice with EAE (unpublished data). Importantly, production of these cytokines was dramatically enhanced in microglia and, to a lesser extent, mDCs when NK cells were depleted (not depicted) or failed to home to the CNS (Table I). In contrast, the differences for TGF-β1 and IL-21 release by microglia and mDCs were not significant (unpublished data). Blocking experiments indeed confirmed the importance of IL-1 and IL-6 for the capacity of microglia to prime Th17 cells (unpublished data).

To investigate the mechanism by which NK cells could influence the capacity of APCs to support Th17 cell differentiation, we cultured naive 2D2 CD62L^{high} cells with mDCs, pDCs, CD8α^{+} DCs, or astrocytes in the presence or absence of NK cells. We found that these APCs, isolated from NK cell–depleted or Cx3cr1$^{-/-}$ mice, exhibited varied capacity

to drive Th17 cell responses (Fig. 5 C). Compared with microglia, the impact of these cells was relatively mild, and NK cells had a minimal influence on their capacity to impact Th17 cell responses (Fig. 5 C). Similar results were obtained with prepolarized Th17 cells (unpublished data).

Considering that microglia were the major source of Th17 cell–polarizing cytokines when NK cells were depleted or failed to home to the CNS (Table I), we hypothesized that the interactions between NK cells and microglia determine the magnitude of CNS inflammation and myelin-reactive Th17 cells. We assessed the capacity of microglia, in the presence or absence of NK cells, to trans-activate the signature transcription factors of the Th17 cell lineage, RORα, RORγ, and STAT3 (Bettelli et al., 2006b; Yang et al., 2008; Zhou et al.,

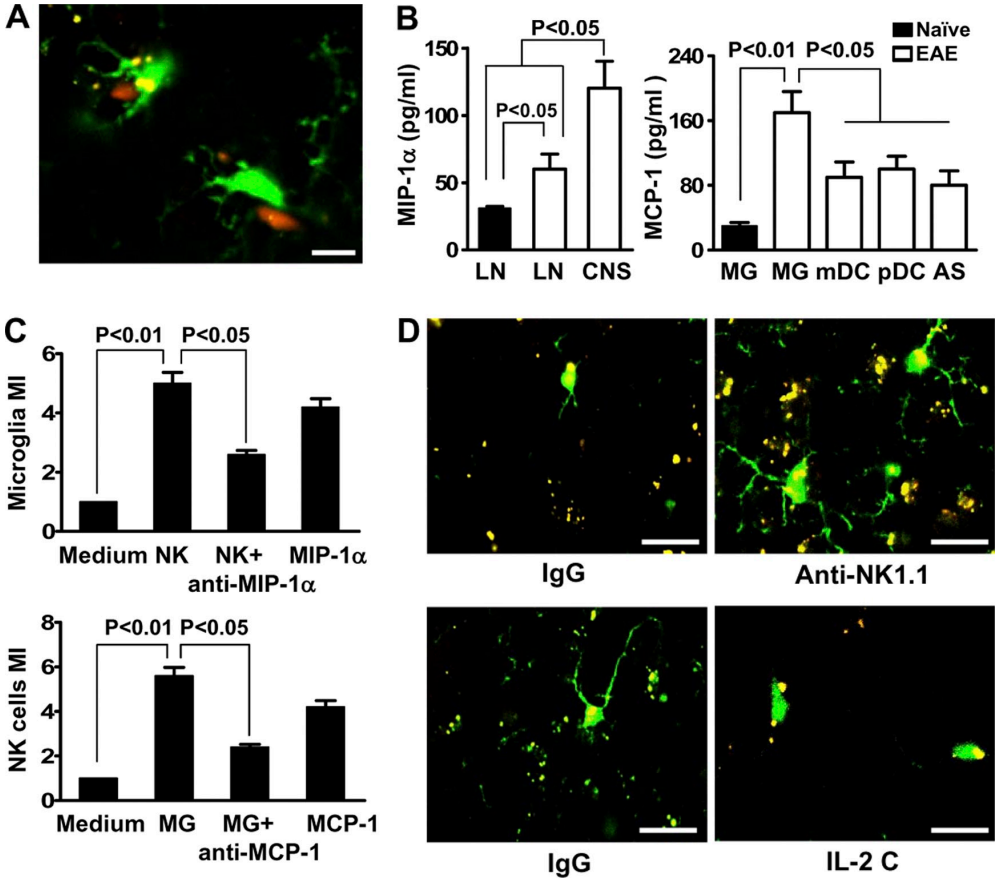

Figure 6. Reciprocal chemoattraction between NK cells and microglia. (A) Colocalization of NK cells and microglia. Cx3cr1$^{GFP+/-}$ mice were immunized with MOG/CFA, brain tissues were harvested during days 12–20 after immunization, and CNS sections were made. NK cells and GFP$^+$ microglia (green) were visualized with anti-NK1.1 or -NKp46 (red). Representative images of four independent experiments with four mice per group each are shown. Bar, 10 µm. (B, left) MIP-1α release by 2 × 10^5 NK cells isolated from lymph node (LN) of naive or MOG-challenged mice and from the CNS during the peak of EAE in mice. (B, right) MCP-1 release from 2 × 10^5 CNS-derived APCs isolated during the peak of EAE. Chemokines were detected by ELISA in cell culture supernatant of the corresponding cells without stimulation. Results are representative of three similar experiments in which cells from 15–20 perfused donor mice were pooled and each APC subset was analyzed three times. Error bars represent the means ± SEM. P-values were determined by an ANOVA test. (C, top) CNS-infiltrating NK cells recruit microglia in an MIP-1α–dependent manner. NK cells induced a substantial recruitment of purified microglia in transwell experiments. Medium only was used as a control. Anti–MIP-1α antibody or MIP-1α was added as indicated. 2 × 10^5 microglia were added to the upper chamber. (C, bottom) Supernatants from microglia recruit NK cells in a MCP-1–dependent manner. Chemotaxis of purified CNS-infiltrating NK cells toward chemokines produced by microglia was tested by using a transwell assay. Supernatants collected from purified microglia were stimulated with PMA and were added to the lower chambers of transwell plates. Medium only was used as a control. Anti–MCP-1 antibody or MCP-1 was added as indicated. 2 × 10^5 NK cells were added to the upper chamber. Specific migration was calculated as migration index. Bars represent means of triplicate wells from a representative of three independent experiments. Error bars represent the means ± SEM. P values were determined by a Student's *t* test. (D) Morphological features of microglia and their proximity to inflammatory foci when NK cells are manipulated. Cx3cr1$^{GFP+/-}$, Cx3cr1$^{-/-}$, and Cx3cr1$^{+/+}$ mice, with microglia labeled with GFP, were immunized with MOG/CFA. A portion of the +/− mice was treated with control IgG, anti-NK1.1 mAb, or IL-2 complexes. Brain tissues were harvested during days 12–20 after immunization. Morphological features of microglia in relation to NK cells were analyzed by confocal microscopy. Activated microglia (increased size of cell body and thickening of proximal processes) were noted at a higher prevalence in control mice. A significantly higher level of reactive oxygen species (ROS; denoting areas of inflammation) was noted in NK cell–deleted mice, whereas the IL-2 complex treatment group had a lower level of ROS compared with control mice. Representative images of three independent experiments with four mice per group each are shown. Bars, 10 µm.

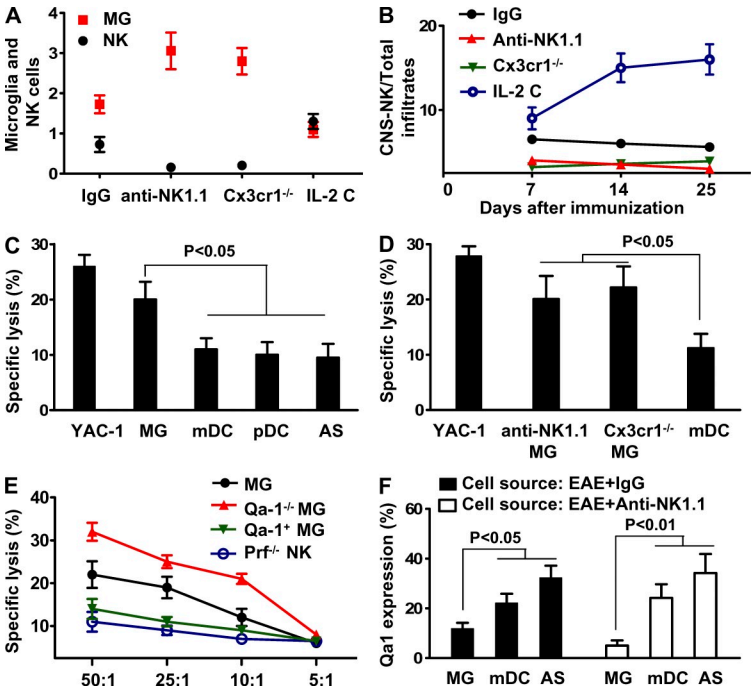

Figure 7. Missing self on microglia breaks NK cell tolerance. (A and B) Inverse relationship between NK cells and microglia. CNS infiltrates were isolated from MOG/CFA-primed Cx3cr1 GFP$^{+/-}$ mice after treatment with control IgG, anti-NK1.1 mAb, or IL-2 complexes. (A) Numbers of NK cells ($\times 10^5$) and GFP$^+$ microglia ($\times 10^6$) that were analyzed by FACS. (B) Ratio of CNS-resident NK cells and total CNS infiltrates. $P < 0.01$ for comparisons of microglial cell numbers from each experimental group with that from control mice. $P < 0.01$ for comparisons of the ratios of CNS-derived NK cells/total infiltrates from the groups that received IL-2 C with that from the remaining groups. $P < 0.05$ for comparisons between groups of mice that received IgG and groups that received anti-NK1.1, or groups of Cx3cr1$^{-/-}$ mice. (C) NK cells principally target microglia. NK cells were purified from pools of CNS tissues harvested from MOG-immunized mice treated with IL-2 complexes. Microglia, astrocytes, mDCs, and pDCs were isolated from MOG-primed Cx3cr1$^{+/-}$ mice and incubated with ^{51}Cr. The effector (NK) and target (microglia) cells (5×10^4) were incubated at E:T ratios of 25:1 and cytolytic effects were measured in a 4-h ^{51}Cr-release assay, as previously described (Shi et al., 2000). (D) Microglia, astrocytes, and mDCs were isolated from MOG-primed Cx3cr1$^{+/-}$ mice or Cx3cr1$^{-/-}$ mice and incubated with ^{51}Cr. The effector (NK) and target (5×10^4) cells were transferred into RAG1$^{-/-}\gamma c^{-/-}$ mice and a rapid elimination assay (see Materials and methods) was performed. (E) Role of the NKG2A–Qa1 pathway in the interaction between NK cells and microglia. Cytotoxicity assay was conducted with effector NK cells from MOG/CFA-primed WT or perforin-deficient mice. Target cell microglia were isolated from Cx3cr1$^{+/-}$ mice, Qa1/Cx3xr1 double-deficient mice (Qa1$^{-/-}$ MG), or with microglia overexpressing Qa1 (Qa-1$^+$ MG). MG denotes microglia isolated from MOG/CFA-primed Cx3cr1$^{-/-}$ mice. Qa1$^+$MG denotes overexpression of Qa1 on microglia from Qa1$^{-/-}$ mice (see Materials and methods). Data regarding the killing activity of NK cells from the CNS of WT animals with EAE were not available, as it was technically challenging to purify sufficient numbers of NK cells to perform the assay. (F) Expression of Qa1 on CNS-derived APCs in the presence or absence of NK cells. CNS-derived cells (days 12–20 after immunization) from MOG-immunized mice treated with IgG or anti-NK1.1 were analyzed for Qa1 expression by FACS. All data are representative of two to three independent experiments with 12–18 mice per group each (mean ± SEM). P-values were determined by an ANOVA test.

2009), in vivo. For this purpose, we isolated microglia, as well as naive or Th17-polarized 2D2 cells (Bettelli et al., 2006a), and transferred these cells into RAG1$^{-/-}\gamma c^{-/-}$ hosts via intracerebral and intravenous routes, respectively. Microglia from Cx3cr1$^{-/-}$ mice and, to a lesser extent, Cx3cr1$^{+/-}$ mice enhanced IL-17 transcripts, together with increases in RORα, RORγ, IRF4 transcripts, and STAT3 expression levels (Fig. 5 D and not depicted). Cotransfer of NK cells derived from CNS tissues largely ablated these effects, and this was largely dependent on perforin expression by NK cells (Fig. 5 D) because transfer of perforin$^{-/-}$ NK cells restored the capacity of microglia to promote Th17 cell expansion (Fig. 5 D). Additionally, transfer of IFN-γ$^{-/-}$ NK cells resulted in a tendency to reduce the effects on microglia (Fig. 5 D). In trying to discriminate whether NK cells acted directly on Th17 cells or whether microglia acted as intermediary target cells, we considered the former possibility less likely because CNS-derived NK cells did not effectively lyse Th17 phenotype cells (unpublished data).

Reciprocal chemoattraction between NK cells and microglia underlies their physical proximity

The preferential impact of NK cells on microglia, among several types of CNS-derived APCs, prompted investigations on the physical relationship between these two cell types. Colocalization studies revealed that NK cells resided in close proximity to microglial cells (Fig. 6 A), whereas such proximity was not evident between NK cells and mDCs, pDCs, or astrocytes (not depicted). Furthermore, CNS-derived NK cells readily produce MIP-1α (Fig. 6 B). Among mDCs, pDCs, astrocytes, and microglia, the latter cells produced MCP-1 (Fig. 6 C). Transwell migration and blocking experiments revealed that production of MIP-1α by NK cells and MCP-1 by microglia resulted in reciprocal chemoattraction of these cells (Fig. 6 C). Additionally, a statistically significant increase was observed in the recruitment of NK cells toward supernatants from microglia, compared with astrocytes, neurons, and other CNS-infiltrating cells (DCs, T cells, and macrophages; unpublished data). In the absence of NK cells in the CNS, microglial cells exhibited dramatic activated morphological features, whereas the opposite was true when NK cells were enriched in the CNS (Fig. 6 D).

Missing self on microglia ablates NK cell tolerance

We assessed the numerical relationship between NK cells and microglia. Although the absolute numbers of CNS-resident NK cells in mice that received IL-2 complexes were slightly higher than in control mice with EAE (Fig. 7 A), the ratio of

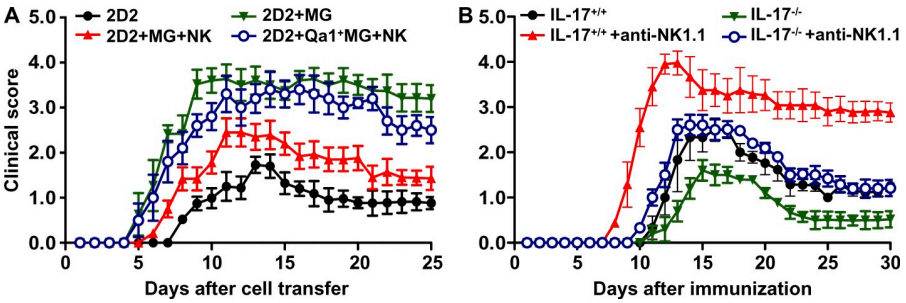

Figure 8. Interactions between NK cells, microglia, and Th17 cells influence the expression of EAE. (A) $CD4^+$ T cells were sorted from the lymph nodes and spleen of 2D2 transgenic mice and cultured under conditions for EAE induction (see Materials and methods). Subsequently, 2×10^5 cells were injected i.v. into MOG/CFA/PT-primed $RAG1^{-/-}$ $\gamma c^{-/-}$ mice. Simultaneously, the same numbers of microglia from $Cx3cr1^{+/-}$ or $Cx3cr1^{-/-}$ mice and NK cells from the IL-2 complex–treated mice were injected into the brain as previously described (Cardona et al., 2006b). In some experiments, Qa1 was overexpressed on microglia with a lentiviral vector (see Materials and methods). Development of EAE in the recipient mice was monitored and compared. $P < 0.05$ after day 10 after cell transfer (Mann-Whitney *U* test) for comparisons between groups receiving 2D2 cells versus 2D2 cells with microglia (except for the group receiving Qa1 overexpressing microglia) and for groups receiving 2D2 cells with microglia versus 2D2 cells with microglia + NK cells. $P > 0.05$ (Mann-Whitney *U* test) at all time points for comparisons among the groups of mice receiving 2D2 cells versus 2D2 cells with microglia and NK cells and for groups receiving untransfected versus Qa1-transfected microglia. $n = 8$–12/group. Error bars represent the means ± SEM. (B) Anti-NK1.1 mAb fails to dramatically alter the course of EAE in IL-17–deficient mice. WT and $IL\text{-}17^{-/-}$ mice were immunized with MOG/CFA. Groups of the immunized mice also received anti-NK1.1 mAb or control IgG (see Materials and methods) upon immunization. Development of EAE was monitored and compared. $P < 0.05$ after day 10 (Mann-Whiteney *U* test) for comparisons between $IL17^{+/+}$ mice that received anti-NK1.1 mAb and all of the other groups. $P > 0.05$ (Mann-Whitney *U* test) at all time points for comparisons among the remaining groups except for $IL\text{-}17^{+/+}$ mice that received anti-NK1.1 mAb. $n = 12$–15/group. Error bars represent the means ± SEM. Data from A and B are pooled from three similar experiments.

CNS-resident NK cells/total CNS infiltrates was 6- to 10-fold higher in mice that received IL-2 complexes, as compared with control mice (Fig. 7 B). The observed inverse relationship between the numbers of NK cells and microglia could be merely a reflection of changes in the intensity of CNS inflammation when NK cells are reduced or enriched. However, the physical proximity between NK cells suggested direct killing of microglia as an alternative possibility. Indeed, among mDCs, pDCs, astrocytes, and microglia, the latter cells were principal targets of NK cells in vitro (Fig. 7 C) and in vivo (Fig. 7 D), and the efficacy of such elimination was abolished when NK cells were isolated from perforin-deficient mice (Fig. 7 E).

The lack of killing by perforin-deficient NK cells suggested that NK cells used cytolytic activity toward microglia during CNS inflammation. In addition to physical factors, loss of the self-MHC class I molecule Qa1 on activated microglia may render these cells key targets for NK cells. Comparisons of expression of Qa1 on APCs from control mice with EAE indicated that levels of Qa1 expression were lower on microglia than on mDCs, pDCs, and astrocytes (Fig. 7 F). Significantly, the differences in Qa1 expression on microglia versus other APCs were greater in NK cell–depleted mice (Fig. 7 F) and in $Cx3cr1^{-/-}$ mice immunized with CFA/MOG (not depicted). Thus, a physical proximity, as well as a reduction in Qa1 expression, ablated NK cell tolerance to microglia, whereas other types of APCs were relatively spared (as a result of maintained Qa1 expression and a relative distance from NK cells).

To further investigate the receptor–ligand pathways that govern interactions between NK cells and microglia, we used two approaches. Qa1 deficiency promoted NK cell killing activity (Fig. 7 E) and diminished the effects of microglia on Th17 cells (Fig. 5 D). Conversely, overexpression of Qa1 protected microglia from NK cell killing (Fig. 7 E) and reduced the influence of NK cells on Th17 cells (Fig. 5 D). As expression of other types of activating and inhibitory NK cell receptors, including NKG2D, Ly49D, CD244 (2B4), Ly49A, and Ly49C, was not dramatically altered upon NK cell homing to the CNS in control and IL-2 complex–treated mice immunized with CFA/MOG (unpublished data), we propose that the NKG2A–Qa1 pathway plays a dominant role in the interactions between NK cells and microglia.

Biological consequences of NK cell–microglia interactions and their dependence on myelin-reactive Th17 cells

Having determined that NK cells suppress the induction of Th17 cell–defining transcription factors that are transactivated by microglia, we sought to address whether this type of interaction between NK cells and microglia can influence the expression of EAE in a cotransfer model. During our initial experiments, we titrated the numbers of 2D2 transgenic T cells, microglia, and NK cells required to induce mild, moderate, and severe EAE in the recipient mice (unpublished data). Because augmentation of myelin-reactive Th17 cells by microglia is anticipated to exacerbate EAE, we decided to use a low number of 2D2 cells to induce mild EAE so that effects of microglia and NK cells on the phenotype of EAE in recipient mice could be easily detected. Transfer of 2D2 cells, along with injection of microglia, resulted in a remarkable augmentation of EAE severity (Fig. 8 A). In contrast, addition of NK cells largely reversed the effect of microglia, and such reversal was abrogated when Qa1 was overexpressed on microglia (Fig. 8 A). Furthermore, the effect of NK cells expanded by IL-2 complexes was dependent on the presence of perforin and, to a lesser extent, IFN-γ, as perforin- and, to a lesser extent, IFN-γ–deficient NK cells lost their capacity to overcome the effect of microglia on EAE (unpublished data).

To further investigate the biological consequences of the interactions between CNS-resident NK cells, microglia, and autoreactive Th17 cells, we used IL-17$^{-/-}$ mice, which are relatively resistant to the development of EAE. Depletion of NK cells from IL-17$^{-/-}$ mice did not significantly alter the EAE phenotype of these animals (Fig. 8 B). Similarly, injection of IL-2 complexes had a minimal effect on the severity of EAE in IL-17$^{-/-}$ mice (unpublished data). Thus, interactions between NK cells, microglia, and Th17 cells play critical roles in determining the phenotype of EAE.

DISCUSSION

Compared with other organ systems, the CNS has several unique properties with respect to immune responses, which includes the spectrum of APCs as well as the neuroimmune microenvironment. Regulatory functions of NK cells in EAE, MS, and other autoimmune diseases have been proposed, but the exact role of NK cells within the CNS remains elusive. Through a combination of approaches using an NK cell–depleting antibody and blockade of NK cell homing to the CNS via disruption of a chemokine receptor that is critical for NK cell recruitment and via expansion of NK cells by IL-2 complexes, we provide compelling evidence that NK cells within the target organ critically control the magnitude of local inflammatory and autoimmune responses against myelin antigens in the CNS. The findings presented in this paper support a dominant role for NK cells in controlling autoimmunity in target organs. First, selective blockade of NK cell homing to the CNS was sufficient to induce unabated pathology in MOG-primed mice. Second, the therapeutic effect of IL-2 complexes was almost entirely dependent on the NK cells in the CNS. Finally, suppression of myelin-reactive Th17 cells (and to some extent Th1 cells) by NK cells was largely restricted to the CNS compartment. Thus, these findings suggest regulatory functions of NK cells within a target organ of autoimmunity, which appears to be more important for disease manifestation than the events that occurred in the periphery (Fig. S7).

The finding that NK cells in the CNS play a more critical role than NK cells in the periphery during CNS inflammation strongly suggests the participation of an additional factor that is specific to the CNS. These factors might include CNS Ags, signals generated from neuronal cells (Tracey, 2009), and CNS-derived APCs. APCs present in the CNS, whether resident or recruited from the periphery, include CD11c^{+} DCs, mDCs, CD8^{+} DCs, astrocytes, and microglia (Olson and Miller, 2004; Greter et al., 2005; Bailey et al., 2007; Weber et al., 2007). Among the different APCs, we found that NK cells preferentially interacted with microglia. The physical proximity of NK cells with microglia, as a result of reciprocal chemoattractions, together with colocalization within inflammatory foci, promoted interactions between these two cell types, and a reduced expression of the MHC class I molecule Qa1 on activated microglia triggered NK cell–mediated cytotoxicity. Altogether, our data suggest that microglia are key targets for NK cells.

NKG2A–Qa1 interactions appeared to play a central role in interactions between NK cells and microglia. In the peripheral lymphoid organs, expression of the inhibitory receptor NKG2A on NK cells is induced by gene products of infectious agents, such as cytomegalovirus, and is sustained by certain cytokines (i.e., IL-12 and IL-10; Sáez-Borderías et al., 2009; Lassen et al., 2010). Interestingly, cytomegalovirus was found to enhance the expression of HLA-E, the human counterpart of Qa1 (Tomasec et al., 2000). Factors that affect the expression of NKG2A on NK cells and Qa1/HLA-E on target cells within the CNS are unknown. In addition to the local inflammatory milieu, CNS-infiltrating NK cells express high levels of nicotinic acetylcholine β2 receptors (unpublished data). Whether these receptors for neuronal or glial transistors, together with other CNS factors, promote expression of NKG2A warrants further investigations.

Activation-induced cell death is an important mechanism to contract the T cell compartment in adaptive immune responses. Under several pathological conditions, such as infections or traumatic injury, NK cells readily home to the brain and spinal cord (Shi and Ransohoff, 2009). Innate NK cells participate in early host defenses and mobilize the adaptive immune system to combat infectious agents. Once infection is controlled, inflammatory responses driven by microglia and other types of CNS-derived APCs must be tapered down to avoid autoimmune responses. By interacting with MHC class I molecules that are constitutively expressed by microglia during steady state and are lost upon prolonged activation, NK cells can ensure tolerance to self while allowing toxicity toward stressed cells.

Microglia are prone to activation (Hanisch and Kettenmann, 2007). Microglia in the CNS are activated in EAE even before the arrival of T cells and other types of peripherally derived APCs (Ponomarev et al., 2007). Future studies will examine whether the temporal activation of microglial cells and other CNS-derived APCs underlies their differential expression of Qa1 to better explain why microglia become targets for NK cells during CNS inflammation.

It must be acknowledged that the precise role of microglia during CNS inflammation is not clear, in part because of technical difficulties in enriching these cells from adult brain tissues. Microglia are capable of performing APC functions upon activation and of priming and inducing final effector T cell functions (Ford et al., 1996; Olson and Miller, 2004; Ponomarev et al., 2005). Activated microglia are thought to play a role in the onset of both MS in humans and EAE in B6 mice (Ponomarev et al., 2007). However, recent studies have provided evidence that microglia are less effective than other APCs in the CNS in presenting myelin antigens and in priming Th cell responses (Bailey et al., 2007). This finding was confirmed in the current model (Fig. 5). We also found that a lack of suppressive effects of NK cells led to an expanded microglia compartment and augmented the capacity of these cells to produce Th17-polarizing cytokines, further suggesting our previous observation that CNS-derived APCs, resident or immigrant, behave differently in the presence or in the absence of NK cells.

NK cell–microglia interactions have a profound impact on myelin-reactive Th cells, particularly the Th17 cell subset. In vivo cell transfer experiments demonstrated that NK cells are capable of abolishing the effects of microglia on the transactivation of the Th17 signature transcription factors RORα, RORγ, and STAT3. It is generally believed that Th cells complete their differentiation in draining lymph nodes (Banchereau and Steinman, 1998). However, chronic CNS inflammation leads to neogenesis of lymphoid structures within the CNS (Magliozzi et al., 2007), which may serve as a structural basis for continued T helper cell differentiation and expansion in this compartment. Participation of microglia clearly indicates that differentiation of autoreactive Th17 cells in the CNS is substantially different from Th17 cell differentiation in the peripheral lymphoid compartment. The importance of NK cell–microglial cell interactions in disease expression during IL-2 complex therapy is illustrated by our cell transfer experiments. Our finding that neither anti-NK1.1 mAbs nor IL-2 complexes significantly altered the course of EAE in IL-17$^{-/-}$ mice further indicates that myelin-reactive Th17 cells are the ultimate targets influenced by interactions between NK cells and microglial cells during CNS inflammation (Fig. 8 B).

NK cells, as well as microglia, have been frequently shown to induce neurotoxicity (Cardona et al., 2006a,b; Hanisch and Kettenmann, 2007). One study has suggested that microglial neurotoxicity is accelerated by the absence of CX3CR1 (Cardona et al., 2006b). Whether lack of CX3CR1 expression, caused by a lack of NK cell recruitment, is responsible for unabated neurotoxicity is unclear. MOG-primed Cx3cr1$^{-/-}$ mice exhibited similar disease phenotype to mice depleted of NK cells, suggesting that a lack of NK cells in the CNS, rather than microglial neurotoxicity, is responsible for the disease phenotype. The temporal, spatial, and specific microenvironment of the CNS and the local cytokine milieu may further influence the detrimental or beneficial effects of NK cells and microglia.

In addition to NK cells, other IL-2R–bearing cells, including NKT cells, CD4$^+$CD25$^+$Foxp3$^+$ regulatory T cells, and CD8$^+$ T cells with a memory phenotype, are also expanded, at various degrees, by IL-2 complexes. Thus, they might as well contribute to disease protection. Although the regulatory functions of CD8$^+$ T cells are less well characterized than those of T reg cells and NKT cells, emerging evidence indicates that a subpopulation of CD8$^+$ T cells can suppress CD4$^+$ T cells (Lu et al., 2008), and mice lacking this CD8$^+$ T cell population can develop exaggerated immune responses to autoantigens (Hu et al., 2004). These cells recognize Qa1 and might use similar mechanisms to NK cells to suppress the functions of microglia (and/or other CNS-derived APCs) or CD4$^+$ T cells, as previously suggested (Lu et al., 2008). Indeed, in our system the IL-2–expanded CD8$^+$ T cells also lysed microglia, albeit at lower efficiency than NK cells, and IL-2 complexes partially lost their therapeutic effects in CD8$^{-/-}$ mice. Whether and how these CD8$^+$ T cells act on other CNS-derived APCs or myelin-reactive T cells directly or indirectly warrants further investigations.

Finally, our findings have important implications for understanding the efficacy of some drugs currently used in CNS disease. For example, daclizumab targets the human IL-2 receptor and inhibits MS and autoimmune uveitis disease activities (Rose et al., 2004, 2007; Li et al., 2005; Bielekova et al., 2006, 2009; Wynn et al., 2010). The efficacy of this drug has been linked to the expansion of CD56^{bright} NK cells (Li et al., 2005; Bielekova et al., 2006, 2009). Copaxone and Rebif/Avonex (IFNs) also increase NK cell cytotoxic activity (Sand et al., 2009; Vandenbark et al., 2009) and the prevalence of CD56^{bright} NK cells, respectively. The IL-2 complexes used in the current studies not only recapitulate the effects of some of these drugs but also provide mechanistic inputs on the importance of CNS versus peripheral NK cells and the means used by NK cells to protect against disease. The importance of CD94/NKG2A-dependent inhibition of myelin-reactive T cells (Lu et al., 2007) and its association with reduced microglia in the CNS during EAE has been elegantly demonstrated (Leavenworth et al., 2010). The current study extends this mechanistic explanation for the contact of NK cells with other types of CNS-derived APCs. Altogether, these studies provide novel insight into the biology of NK cells in relation to organ-specific autoimmunity and might lead to the design of NK cell–based approaches for intervention in inflammatory and autoimmune disorders of the CNS.

MATERIALS AND METHODS

Mice. Female C57BL/6 (B6, H-2^b) mice were purchased from Taconic, and 2D2 mice (Bettelli et al., 2006a) and IL-17$^{-/-}$ mice (Komiyama et al., 2006) were provided by V. Kuchroo (Brigham and Women's Hospital and Harvard Medical School, Boston, MA) and Y. Iwakura (University of Tokyo, Tokyo, Japan), respectively. Other mutant mice, including Cx3cr1$^{GFP/GFP}$ (Cx3cr1$^{-/-}$; Jung et al., 2000), Qa1$^{-/-}$, CD1d$^{-/-}$, RAG1$^{-/-}$γc$^{-/-}$, perforin$^{-/-}$, and IFN-γ$^{-/-}$ mice were either available in our colony or purchased from The Jackson Laboratory. All mutant mice were backcrossed to the B6 background for 8–12 generations and were housed in pathogen-free conditions at animal facilities of the Barrow Neurological Institute (Phoenix, AZ) or the Tianjin Neurological Institute (Tianjin, China). All animal studies were approved by Animal Care and Use Committees of the Barrow-St. Joseph and Tianjin Neurological Institute.

EAE model. The mouse peptide autoantigen MOG$_{35-55}$ (M-E-V-G-W-Y-R-S-P-F-S-R-V-V-H-L-Y-R-N-G-K) was synthesized (purity > 95%) by Bio Synthesis Inc. To induce acute EAE, B6 mice were injected s.c. in the hind flank with 200 μg MOG$_{35-55}$ peptide in CFA (BD) containing 500 μg of nonviable dessicated *Mycobacterium tuberculosis*. On the day of, and 2 d after, immunization, the mice were also inoculated with 200 ng pertussis toxin (List Biological) i.v. The passive transfer EAE model with 2D2 T cells is detailed in the Fig. 8 legend. In brief, splenocytes from MOG TCR transgenic (2D2) mice were stimulated with 10 μg/ml MOG$_{35-55}$ for 48 h and then expanded in 5 ng/ml IL-2 and IL-7 for 5 d. The lymphoblasts were stimulated with 1 μg/ml of plate-bound anti-CD3 and 1 μg/ml of anti-CD28 in the presence of 10 ng/ml IL-12 and 25 ng/ml IL-18 for 24 h. Depending on the experiments, 2 × 10^5–10^6 2D2 T cells were transferred into RAG1$^{-/-}$γc$^{-/-}$ mice by i.v. injection. Clinical presentations in both models were assessed as previously described (Huang et al., 2006).

In vivo antibody and cytokine administration. mAbs directed against mouse NK1.1 (PK136 clone; Koo and Peppard, 1984), IL-2 (S4B6 clone), and CD25 (PC61) were produced from hybridomas (American Type Culture Collection). Carrier-free recombinant mouse IL-2 was purchased from eBioscience. Mouse IgG2a (Sigma-Aldrich) was used as the isotype control antibody.

For depletion of NK1.1$^+$ cells or CD25$^+$ cells in vivo, 100 µg of anti-NK1.1 mAb or anti-CD25 mAb was injected i.p. into each mouse at day −2 after immunization. Every 5 d thereafter, 50 µg anti-NK1.1 mAb or anti-CD25 were injected i.p. until termination of experiments (Shi et al., 2000; Liu et al., 2005). Depletion of NK1.1$^+$ and CD25$^+$ cells was confirmed by flow cytometry and was always >90%.

For the preparation and administration of IL-2 and anti–IL-2 mAb complexes (referred to as IL-2 complexes), equal volumes of 30 µg/ml rIL-2 and 300 µg/ml of anti–mouse IL-2 mAb in PBS were mixed in vitro and 100 µl of this solution was injected i.p. into each mouse, resulting in IL-2 complexes formed by 1.5 µg rIL-2 with 15 µg of anti–IL-2 mAb per mouse, as modified from a published protocol (Boyman et al., 2006). As controls, animals were treated with rIL-2 or anti–IL-2 mAb only and received 200 µl IgG with the same amount of either rIL-2 or anti–IL-2 mAb as for the IL-2 complexes. Additional control mice received equivalent doses of purified normal rat isotype IgG2a. Injections were repeated two times every week starting on the same day of MOG_{35-55} immunization (day 0) until termination of the experiment.

Intracerebral injection. Mice were anesthetized with 87 mg/kg ketamine and 13 mg/kg xylazine and placed in the stereotaxic apparatus (Kopf Instruments). Microglia injection was performed as previously described (Cardona et al., 2006b). Implantation was performed as previously described with some modifications (see Supplemental material; Abizaid et al., 2006; Hemsley et al., 2009).

Neuropathology and neuroimaging. For study of inflammation, GFP$^+$ microglia morphology, cellular colocalization, and dihydroethidium (DHE) oxidation in mice brain, mice received DHE i.p. and were sacrificed by pentobarbital injection 18 h later and perfused by intracardiac puncture with 50 ml of cold PBS. Brains and spinal cords were removed, frozen immediately, and then stored at −80°C. 10–30-µm serial cryosections were prepared. Three serial sections were stained with H&E, luxol blue, PE anti-NK1.1 (PK136), or anti-NKp46 (29A1.4) antibodies. All images were captured with a confocal microscope (LSM 710; Carl Zeiss, Inc.) with Microscope image acquisition software.

For imaging of ROS generation in brain, bioluminescence images in live mice were captured using the Xenogen IVIS200 imager (Caliper Life Sciences) at several time points after injection of 27 mg/kg DHE (Invitrogen). A region of interest tool was used to measure the fluorescent intensity. Data were collected as photons per second per centimeter squared using the Living Image software (Caliper Life Sciences).

MRI was performed using a 7T small animal, 30-cm horizontal-bore magnet, and BioSpec Avance III spectrometer (Bruker) with a 116-mm high power gradient set (600 mT/m) and a 72-mm whole-body mouse transmit/surface receive coil configuration. Axial and coronal T1-weighted (MSME; echo time [TE] 10.5 ms, repetition time [TR] 322 ms, 0.5-mm slice thickness, matrix 256 × 256, field of view [FOV] 2.8 cm, eight averages, 40 coronal slices, scan time 22 min, and 20 axial slices, scan time 16 min) and fat-suppressed turbo spin echo T2-weighted (RARE; TE1 14.5 ms, TE2 65.5 ms, TR 4,500 ms, 0.5-mm slice thickness, Matrix 256 × 256, FOV 2.8 cm, eight averages, 40 coronal slices, scan time 28 min, and 20 axial slices, scan time 28 min) images were acquired, covering the volume of brain from the olfactory bulb/frontal lobe fissure to the cervical spinal cord. MRI data were analyzed using the MEDx3.4.3 software package (Medical Numerics) on a LINUX workstation.

Isolation of mononuclear cells from the CNS. For CNS-infiltrating mononuclear cell isolation, at day 11 after EAE induction mice were sacrificed and perfused with PBS delivered transcardially to eliminate contaminating blood cells in the CNS. Fresh brain and/or spinal cords were removed from five to six mice, cut into small pieces, and digested in 10 mM Hepes/NaOH buffer containing 1 mg/ml collagenase for 1 h at 37°C. Tissues were homogenized with a syringe, filtered through a 70-µM cell strainer to obtain a single cell suspension, and centrifuged. Cell pellets were resuspended in 30% percoll and centrifuged against 70% percoll. The cell monolayer between the 30–70% percoll interface was collected as the CNS mononuclear cells for staining. APCs (mDC, CD45^{hi}CD3ε$^-$CD11b$^+$F4/80$^+$CD11c$^+$; pDC, CD11b$^-$CD11c$^+$B220$^+$PDCA-1$^+$CD8α$^+$ or CD8α$^-$ and CD11b$^-$CD11c$^+$B220$^-$CD8α$^+$CD205$^+$ or CD205$^-$CD8α$^+$ DCs; astrocytes, GFAP) were isolated and enriched as previously described with modification (Bailey et al., 2007; Liu et al., 2007). For cytokine induction, the isolated CNS-derived APCs were cultured with 3 ng/ml GM-CSF (R&D Systems). 1 µg/ml of soluble CD40L (R&D Systems) was added. After 48 h, IL-1, IL-6, IL-21, TGF-β, and IL-23 in the supernatant was assayed by ELISA according to the manufacturer's instructions (eBioscience).

Microglial cell isolation. We used mice in which the CX3CR1 gene was replaced with a cDNA encoding GFP, such that Cx3cr1$^{+/-}$ (Cx3cr1$^{+/GFP}$) mice express the GFP reporter in cells that retain their receptor function, whereas Cx3cr1$^{-/-}$ (Cx3cr1$^{GFP/GFP}$) cells are also labeled and lack CX3CR1 expression (Cardona et al., 2006a,b). Because CX3CR1-GFP reporter mice can exclusively identify microglia in vivo in the CNS, the Cx3cr1$^{+/-}$ mice permitted us to isolate and purify these cells ex vivo (Cardona et al., 2006a,b). Before removal of CNS tissues, perfusion was routinely performed to exclude contamination of peripherally arrived cells also expressing CX3CR1 (also GFP$^+$).

Construction of lentiviral vectors encoding Qa-1 and transduction into microglia. Full-length Qa-1 cDNA was amplified by RT-PCR from RNA isolated from splenocytes of B6 mice. After verification of the sequence, cDNA was ligated into the Plvx-DsRed-Monomer-C1 vector (Takara Bio Inc.) replacing the red protein coding sequence of DsRed. The recombinant lentivirus was produced by Lenti-X 293T Cells (Takara Bio Inc.) with Lenti-X HT Packaging System (Takara Bio Inc.). Virus was collected 72 h after transfection and titers were up to 5–8 × 10^8 infectious units/ml. Microglia purified from B6 background Qa-1–deficient mice were infected with virus in 24-well plates precoated with 20 µg/ml poly-L-lysine for 16 h. The virus-containing transduction medium was then replaced with fresh growth medium, the incubation of the cells continued for 24 h at 37°C and 5% CO_2.

NK cell cytotoxicity assays. NK cell cytotoxicity was assessed by the chromium release assay using ^{51}Cr-labeled YAC-1 mouse lymphoma cell line, microglia, and other types of APCs (Shi et al., 2000). Freshly purified NK cells were incubated with ^{51}Cr-labeled target cells (5 × 10^3) at various effector cell/target cell ratios. After 4 h of incubation, the supernatants were harvested and ^{51}Cr release was measured with a γ counter (PerkinElmer). The percentage of specific lysis was calculated according to the following formula: (experimental release − spontaneous release)/(maximum release − spontaneous release) × 100. Cytotoxicity assay was done in triplicate (Shi et al., 2000).

A rapid elimination assay was used to determine whether NK cells can eliminate microglia in vivo, as previously described (Assarsson et al., 2004). 5 × 10^5 ^{51}Cr-labeled microglia were microinjected into the brain of the recipient mice. The CNS tissues (brain and spinal cord) were removed after 8 h and counted in a gamma radiation counter. The percentage of remaining radioactivity was determined as follows: (organ − background/dose of cells − background) × 100. Radioactivity recovered from control mice and experimental mice was an accurate measurement of intact microglia remaining in the CNS.

Cell migration assay. Chemotaxis of microglia toward chemokines produced by CNS-derived NK cells was tested in vitro using a polycarbonate filter microchamber filtration system (Neuro Probe) with small pores (3 µm). 2 × 10^5 microglial cells were added to the upper well of the upper compartment in the presence of 1 nM PMA. The lower compartment was filled with 300 µl of medium containing no chemotactic supplement, recombinant 10 ng/ml MIP-1α (R&D Systems), or supernatants collected from purified microglia cells stimulated for 24 h with 1 nM PMA with or without 5 µg/m of anti–MIP-1α (R&D Systems). Chemotaxis of CNS-derived NK cells toward chemokines produced by microglia was tested using the same system. In brief, 2 × 10^5 NK cells were seeded into the upper compartment of the

microchamber system with 100 U/ml IL-2. Lower chambers were filled with 300 µl of supernatant from purified microglial cells stimulated for 24 h with 1 nM PMA (Sigma-Aldrich) with or without 5 µg/ml of anti–MCP-1 antibody (BD). Medium only or with 10 ng/ml of recombinant MCP-1 (R&D Systems) was used as control.

After 2 h, the migrated cells indicated above were harvested from the lower compartment of the chemotaxis chamber and analyzed by flow cytometry. Staining with PI confirmed that >95% of the migrated cells were viable. Migration index (MI) was calculated as follows: MI = (number of cells migrating toward chemokine)/(number of cells migrating toward medium alone).

Cell proliferation (CFSE and BrdU) assays. For CFSE labeling assays, single cell suspensions (4×10^7 cells) were prepared and labeled with 0.5 µM CFSE at 37°C for 10 min. Subsequently, when cells were cultured, levels of CFSE staining declined with each cell division, allowing for cell proliferation to be monitored. Cells labeled with or without CFSE were incubated at 37°C for 3 d in round-bottom plates (2×10^6 cells/well) with or without antigens (10 µg/ml MOG_{35-55}). After harvesting, cells were stained for surface markers with fluorochrome-conjugated monoclonal antibodies, including anti–CD3-PE/Cy5 (17A2), anti–CD4-allophycocyanin/Cy7 (GK1.5), and anti–CD8α-PE/Cy7 (53–6.7; BD). Isotype-matched monoclonal antibodies were used as controls.

For in vivo BrdU incorporation assays, mice were injected with 1.0 mg BrdU (BD) solution. After 18–24 h, single cell suspensions were prepared from spleens and/or thymuses and surface stained with PE-Cy7–labeled anti-CD4 (GK1.4), allophycocyanin-labeled anti-CD25 (7D4), and FITC-labeled anti-BrdU mAb according to the manufacturer's instructions (BD). Samples were analyzed on a FACSAria flow cytometer (BD) using Diva software.

FACS analysis. Single cell suspensions (10^6 cells) were prepared from spleen or lymph nodes or CNS and stained with fluorochrome-conjugated antibodies. All antibodies were purchased from BD, eBioscience, or Santa Cruz Biotechnology, Inc. unless otherwise indicated. Antibodies were directly labeled with one of the following fluorescent tags: FITC, PE, PerCP, allophycocyanin, PC5, or PC7. The following antibodies were used: CD3 (145-2C11), CD4 (GK1.4), CD8 (53–6.7), CD11b (M1/70), CD11c (HL3), CD19 (1D3), CD25 (7D4), CD38 (90), CD138 (281–2), STAT3 (pY705), Qa1 (6A8.6F10), NKG2D (CX5), NKp46 (29A1.4), F4/80 (BM8), CD205 (205yekta), and NK1.1 (PK136). Flow cytometric data were collected on a FACSAria flow cytometer and analyzed with Diva software. Isotype-matched negative control mAbs were used for all stains. To determine the percentage of cells producing selected cytokines, values obtained with isotype controls were subtracted from those with specific mAb.

Cytokine quantification. For intracellular cytokine staining, single cell suspensions ($\sim 30 \times 10^6$ cells) were prepared and incubated at 37°C for 4 d in round-bottom plates (2×10^6 cells/well) with or without antigens (10 µg/ml MOG_{35-55} or 5 µg/ml Con A) and stimulated with a mixture of 20 ng/ml PMA, 1 µg/ml ionomycin, and 5 µg/ml brefeldin A for another 5 h at 37°C. After harvesting, cells were stained for surface markers, fixed and permeabilized with the Cytofix/Cytoperm kit (BD), and then stained with anti–IFN-γ and anti–IL-17 mAb conjugated with Alexa Fluor 647 or PE. For intracellular Foxp3 expression, fresh cells were stained for surface markers with anti–CD4-FITC (H129.19) and anti–CD25-allophycocyanin (PC61.5) for 15 min at 4°C, fixed, permeabilized, and then stained with anti–Foxp3-PE (FJK-16s; eBioscience). All samples were analyzed on a FACSAria using Diva software. ELISA with OptEIA kits (BD) was performed for assessment of cytokine release from microglia and IL-2 complex-expanded NK cells.

qRT-PCR. Total RNA was extracted from cell suspensions of spinal cords using TRIzol (Invitrogen). First-strand cDNA of each sample was synthesized using a reverse transcription kit (Invitrogen). RT-PCR was performed as previously described, using an ABI Prism 7900-HT sequence system (Applied Biosystems) with the QuantiTect SYBR Green PCR kit (QIAGEN), in accordance with the manufacturer's instructions. The following primers were used: IL-17 forward, 5′-CCTCCAGAATGTGAAGGTCA-3′; IL-17 reverse, 5′-CTATCAGGGTCTTCATTGCG-3′; IFN-γ forward, 5′-AGCTCTTCCTCATGGCTGTT-3′; IFN-γ reverse, 5′-TTTGCCAGTTCCTCCAGATA-3′; RORα forward, 5′-TCTCCCTGCGCTCTCCGCAC-3′; RORα reverse, 5′-TCCACAGATCTTGCATGGA-3′; RORγ forward, 5′- CCCCCTGCCCAGAAACACT-3′; RORγ reverse, 5′-GGATGCCCCCATTCACTTACTTCT-3′; hypoxanthine-guanine phosphoribosyltransferase (HPRT) forward, 5′-AGCCTAAGATGAGCGCAAGT-3′; and HPRT reverse, 5′-TTACTAGGCAGATGGCCACA-3′. The HPRT gene was amplified and served as an endogenous control. 1 µl of first-strand cDNA product was amplified with platinum Taq polymerase (Invitrogen) and gene-specific primer pairs. Each sample was assayed in triplicate and experiments were repeated twice. The relative amounts of mRNA were calculated by plotting the Ct (cycle number), and mean relative expression was determined by the $2^{-\Delta\Delta Ct}$ comparative method.

Online supplemental material. Fig. S1 shows approaches to study NK cells during CNS inflammation. Fig. S2 shows the effect of anti-NK1.1 mAb on the development and progression of EAE in B6 mice and in $CD1d^{-/-}$ mice. Fig. S3 shows global alteration of Th17-polarizing cytokines and other inflammatory mediators in mice when NK cells are manipulated. Fig. S4 shows the impact of anti-NK1.1 mAb or IL-2 C injection on $CD8^+$ T cell responses. Fig. S5 shows effects of IL-2 immune complexes on NK ($CD3^-NK1.1^+$), NKT ($CD3^+NK1.1^+$), $CD4^+$, $CD4^+CD25^+$, and $CD4^+CD25^+$T cells. Fig. S6 shows the contributions of IL-2 receptor–bearing NKT cells, T reg cells, and $CD8^+$ cells to protection against EAE conferred by IL-2 complexes. Fig. S7 shows NK cell–mediated inhibition of Th17 cells and autoimmunity in the CNS. Table S1 shows the effects of IL-2 complexes on induction and maintenance of NK cells, as well as clinical features of EAE. Online supplemental material is available at http://www.jem.org/cgi/content/full/jem.20092749/DC1.

We thank Drs. D. Huang and R. Ransohoff for collaborations on early experiments performed with $Cx3cr1^{GFP/GFP}$ mice, C. Dong and H.G. Ljunggren for discussions, V. K. Kuchroo for 2D2 mice, Y. Iwakura for $IL\text{-}17^{-/-}$ mice, G. Turner for support on 7T MRI, and S. Rhodes, D. Dayao, and S. Shi for technical support.

This study was supported in part by the National Natural Science Foundation of China (F.D. Shi), Arizona Biomedical Research Commission (9-140 to F.D. Shi), and the National Institutes of Health (AI083294 to F.D. Shi; AR53293 to A. La Cava; AI070305 and HL089667 to L. Van Kaer). J. Hao is supported by China Scholarship Council 2008622008. R. Liu is a Hobb Family Neuroimmunology Fellow.

The authors disclosed no financial conflicts of interest.

Submitted: 24 December 2009
Accepted: 6 July 2010

REFERENCES

Abizaid, A., Z.W. Liu, Z.B. Andrews, M. Shanabrough, E. Borok, J.D. Elsworth, R.H. Roth, M.W. Sleeman, M.R. Picciotto, M.H. Tschöp, et al. 2006. Ghrelin modulates the activity and synaptic input organization of midbrain dopamine neurons while promoting appetite. *J. Clin. Invest.* 116:3229–3239. doi:10.1172/JCI29867

Assarsson, E., T. Kambayashi, J.D. Schatzle, S.O. Cramer, A. von Bonin, P.E. Jensen, H.G. Ljunggren, and B.J. Chambers. 2004. NK cells stimulate proliferation of T and NK cells through 2B4/CD48 interactions. *J. Immunol.* 173:174–180.

Bailey, S.L., B. Schreiner, E.J. McMahon, and S.D. Miller. 2007. CNS myeloid DCs presenting endogenous myelin peptides 'preferentially' polarize CD4+ T(H)-17 cells in relapsing EAE. *Nat. Immunol.* 8: 172–180. doi:10.1038/ni1430

Banchereau, J., and R.M. Steinman. 1998. Dendritic cells and the control of immunity. *Nature.* 392:245–252. doi:10.1038/32588

Bettelli, E., D. Baeten, A. Jäger, R.A. Sobel, and V.K. Kuchroo. 2006a. Myelin oligodendrocyte glycoprotein-specific T and B cells cooperate to induce a Devic-like disease in mice. *J. Clin. Invest.* 116:2393–2402. doi:10.1172/JCI28334

Bettelli, E., Y. Carrier, W. Gao, T. Korn, T.B. Strom, M. Oukka, H.L. Weiner, and V.K. Kuchroo. 2006b. Reciprocal developmental pathways for the generation of pathogenic effector TH17 and regulatory T cells. *Nature*. 441:235–238. doi:10.1038/nature04753

Bielekova, B., M. Catalfamo, S. Reichert-Scrivner, A. Packer, M. Cerna, T.A. Waldmann, H. McFarland, P.A. Henkart, and R. Martin. 2006. Regulatory CD56(bright) natural killer cells mediate immunomodulatory effects of IL-2Ralpha-targeted therapy (daclizumab) in multiple sclerosis. *Proc. Natl. Acad. Sci. USA*. 103:5941–5946. doi:10.1073/pnas.0601335103

Bielekova, B., T. Howard, A.N. Packer, N. Richert, G. Blevins, J. Ohayon, T.A. Waldmann, H.F. McFarland, and R. Martin. 2009. Effect of anti-CD25 antibody daclizumab in the inhibition of inflammation and stabilization of disease progression in multiple sclerosis. *Arch. Neurol.* 66:483–489. doi:10.1001/archneurol.2009.50

Biron, C.A., K.B. Nguyen, G.C. Pien, L.P. Cousens, and T.P. Salazar-Mather. 1999. Natural killer cells in antiviral defense: function and regulation by innate cytokines. *Annu. Rev. Immunol.* 17:189–220. doi:10.1146/annurev.immunol.17.1.189

Boyman, O., M. Kovar, M.P. Rubinstein, C.D. Surh, and J. Sprent. 2006. Selective stimulation of T cell subsets with antibody-cytokine immune complexes. *Science*. 311:1924–1927. doi:10.1126/science.1122927

Cardona, A.E., D. Huang, M.E. Sasse, and R.M. Ransohoff. 2006a. Isolation of murine microglial cells for RNA analysis or flow cytometry. *Nat. Protoc.* 1:1947–1951. doi:10.1038/nprot.2006.327

Cardona, A.E., E.P. Pioro, M.E. Sasse, V. Kostenko, S.M. Cardona, I.M. Dijkstra, D. Huang, G. Kidd, S. Dombrowski, R. Dutta, et al. 2006b. Control of microglial neurotoxicity by the fractalkine receptor. *Nat. Neurosci.* 9:917–924. doi:10.1038/nn1715

Chambers, B.J., M. Salcedo, and H.G. Ljunggren. 1996. Triggering of natural killer cells by the costimulatory molecule CD80 (B7-1). *Immunity*. 5:311–317. doi:10.1016/S1074-7613(00)80257-5

Feuerer, M., Y. Shen, D.R. Littman, C. Benoist, and D. Mathis. 2009. How punctual ablation of regulatory T cells unleashes an autoimmune lesion within the pancreatic islets. *Immunity*. 31:654–664. doi:10.1016/j.immuni.2009.08.023

Ford, A.L., E. Foulcher, F.A. Lemckert, and J.D. Sedgwick. 1996. Microglia induce CD4 T lymphocyte final effector function and death. *J. Exp. Med.* 184:1737–1745. doi:10.1084/jem.184.5.1737

French, A.R., and W.M. Yokoyama. 2004. Natural killer cells and autoimmunity. *Arthritis Res. Ther.* 6:8–14. doi:10.1186/ar1034

Greter, M., F.L. Heppner, M.P. Lemos, B.M. Odermatt, N. Goebels, T. Laufer, R.J. Noelle, and B. Becher. 2005. Dendritic cells permit immune invasion of the CNS in an animal model of multiple sclerosis. *Nat. Med.* 11:328–334. doi:10.1038/nm1197

Hanisch, U.K., and H. Kettenmann. 2007. Microglia: active sensor and versatile effector cells in the normal and pathologic brain. *Nat. Neurosci.* 10:1387–1394. doi:10.1038/nn1997

Hemsley, K.M., A.J. Luck, A.C. Crawley, S. Hassiotis, H. Beard, B. King, T. Rozek, T. Rozaklis, M. Fuller, and J.J. Hopwood. 2009. Examination of intravenous and intra-CSF protein delivery for treatment of neurological disease. *Eur. J. Neurosci.* 29:1197–1214. doi:10.1111/j.1460-9568.2009.06666.x

Hu, D., K. Ikizawa, L. Lu, M.E. Sanchirico, M.L. Shinohara, and H. Cantor. 2004. Analysis of regulatory CD8 T cells in Qa-1-deficient mice. *Nat. Immunol.* 5:516–523. doi:10.1038/ni1063

Huang, D., F.D. Shi, S. Jung, G.C. Pien, J. Wang, T.P. Salazar-Mather, T.T. He, J.T. Weaver, H.G. Ljunggren, C.A. Biron, et al. 2006. The neuronal chemokine CX3CL1/fractalkine selectively recruits NK cells that modify experimental autoimmune encephalomyelitis within the central nervous system. *FASEB J.* 20:896–905. doi:10.1096/fj.05-5465com

Jung, S., J. Aliberti, P. Graemmel, M.J. Sunshine, G.W. Kreutzberg, A. Sher, and D.R. Littman. 2000. Analysis of fractalkine receptor CX(3)CR1 function by targeted deletion and green fluorescent protein reporter gene insertion. *Mol. Cell. Biol.* 20:4106–4114. doi:10.1128/MCB.20.11.4106-4114.2000

Kärre, K., H.G. Ljunggren, G. Piontek, and R. Kiessling. 1986. Selective rejection of H-2-deficient lymphoma variants suggests alternative immune defence strategy. *Nature*. 319:675–678. doi:10.1038/319675a0

Komiyama, Y., S. Nakae, T. Matsuki, A. Nambu, H. Ishigame, S. Kakuta, K. Sudo, and Y. Iwakura. 2006. IL-17 plays an important role in the development of experimental autoimmune encephalomyelitis. *J. Immunol.* 177:566–573.

Koo, G.C., and J.R. Peppard. 1984. Establishment of monoclonal anti-Nk-1.1 antibody. *Hybridoma*. 3:301–303. doi:10.1089/hyb.1984.3.301

Lanier, L.L. 2008. Up on the tightrope: natural killer cell activation and inhibition. *Nat. Immunol.* 9:495–502. doi:10.1038/ni1581

Laouar, Y., F.S. Sutterwala, L. Gorelik, and R.A. Flavell. 2005. Transforming growth factor-beta controls T helper type 1 cell development through regulation of natural killer cell interferon-gamma. *Nat. Immunol.* 6:600–607. doi:10.1038/ni1197

Lassen, M.G., J.R. Lukens, J.S. Dolina, M.G. Brown, and Y.S. Hahn. 2010. Intrahepatic IL-10 maintains NKG2A+Ly49- liver NK cells in a functionally hyporesponsive state. *J. Immunol.* 184:2693–2701. doi:10.4049/jimmunol.0901362

Leavenworth, J.W., C. Schellack, H.J. Kim, L. Lu, P. Spee, and H. Cantor. 2010. Analysis of the cellular mechanism underlying inhibition of EAE after treatment with anti-NKG2A F(ab')2. *Proc. Natl. Acad. Sci. USA*. 107:2562–2567. doi:10.1073/pnas.0914732107

Li, Z., W.K. Lim, S.P. Mahesh, B. Liu, and R.B. Nussenblatt. 2005. Cutting edge: in vivo blockade of human IL-2 receptor induces expansion of CD56(bright) regulatory NK cells in patients with active uveitis. *J. Immunol.* 174:5187–5191.

Liu, J.Q., J.W. Carl Jr., P.S. Joshi, A. RayChaudhury, X.A. Pu, F.D. Shi, and X.F. Bai. 2007. CD24 on the resident cells of the central nervous system enhances experimental autoimmune encephalomyelitis. *J. Immunol.* 178:6227–6235.

Lu, L., K. Ikizawa, D. Hu, M.B. Werneck, K.W. Wucherpfennig, and H. Cantor. 2007. Regulation of activated CD4+ T cells by NK cells via the Qa-1-NKG2A inhibitory pathway. *Immunity*. 26:593–604. doi:10.1016/j.immuni.2007.03.017

Lu, L., H.J. Kim, M.B. Werneck, and H. Cantor. 2008. Regulation of CD8+ regulatory T cells: Interruption of the NKG2A-Qa-1 interaction allows robust suppressive activity and resolution of autoimmune disease. *Proc. Natl. Acad. Sci. USA*. 105:19420–19425. doi:10.1073/pnas.0810383105

Liu, R., A. La Cava, X.F. Bai, Y. Jee, M. Price, D.I. Campagnolo, P. Christadoss, T.L. Vollmer, L. Van Kaer, and F.D. Shi. 2005. Cooperation of invariant NKT cells and CD4+CD25+ T regulatory cells in the prevention of autoimmune myasthenia. *J. Immunol.* 175:7898–7904.

Magliozzi, R., O. Howell, A. Vora, B. Serafini, R. Nicholas, M. Puopolo, R. Reynolds, and F. Aloisi. 2007. Meningeal B-cell follicles in secondary progressive multiple sclerosis associate with early onset of disease and severe cortical pathology. *Brain*. 130:1089–1104. doi:10.1093/brain/awm038

Martín-Fontecha, A., L.L. Thomsen, S. Brett, C. Gerard, M. Lipp, A. Lanzavecchia, and F. Sallusto. 2004. Induced recruitment of NK cells to lymph nodes provides IFN-gamma for T(H)1 priming. *Nat. Immunol.* 5:1260–1265. doi:10.1038/ni1138

Mendiratta, S.K., W.D. Martin, S. Hong, A. Boesteanu, S. Joyce, and L. Van Kaer. 1997. CD1d1 mutant mice are deficient in natural T cells that promptly produce IL-4. *Immunity*. 6:469–477. doi:10.1016/S1074-7613(00)80290-3

O'Garra, A. 1998. Cytokines induce the development of functionally heterogeneous T helper cell subsets. *Immunity*. 8:275–283. doi:10.1016/S1074-7613(00)80533-6

Olson, J.K., and S.D. Miller. 2004. Microglia initiate central nervous system innate and adaptive immune responses through multiple TLRs. *J. Immunol.* 173:3916–3924.

Ponomarev, E.D., L.P. Shriver, K. Maresz, and B.N. Dittel. 2005. Microglial cell activation and proliferation precedes the onset of CNS autoimmunity. *J. Neurosci. Res.* 81:374–389. doi:10.1002/jnr.20488

Ponomarev, E.D., L.P. Shriver, K. Maresz, J. Pedras-Vasconcelos, D. Verthelyi, and B.N. Dittel. 2007. GM-CSF production by autoreactive T cells is required for the activation of microglial cells and the onset of experimental autoimmune encephalomyelitis. *J. Immunol.* 178:39–48.

Raulet, D.H. 2004. Interplay of natural killer cells and their receptors with the adaptive immune response. *Nat. Immunol.* 5:996–1002. doi:10.1038/ni1114

Rose, J.W., H.E. Watt, A.T. White, and N.G. Carlson. 2004. Treatment of multiple sclerosis with an anti-interleukin-2 receptor monoclonal antibody. *Ann. Neurol.* 56:864–867. doi:10.1002/ana.20287

Rose, J.W., J.B. Burns, J. Bjorklund, J. Klein, H.E. Watt, and N.G. Carlson. 2007. Daclizumab phase II trial in relapsing and remitting multiple sclerosis: MRI and clinical results. *Neurology*. 69:785–789. doi:10.1212/01.wnl.0000267662.41734.1f

Sáez-Borderías, A., N. Romo, G. Magri, M. Gumá, A. Angulo, and M. López-Botet. 2009. IL-12-dependent inducible expression of the CD94/NKG2A inhibitory receptor regulates CD94/NKG2C+ NK cell function. *J. Immunol.* 182:829–836.

Sand, K.L., E. Knudsen, J. Rolin, Y. Al-Falahi, and A.A. Maghazachi. 2009. Modulation of natural killer cell cytotoxicity and cytokine release by the drug glatiramer acetate. *Cell. Mol. Life Sci.* 66:1446–1456. doi:10.1007/s00018-009-8726-1

Shi, F.D., and R. Ransohoff. 2010. Nature Killer Cells in the Central Nervous System. *In* Natural Killer Cells. M.T. Lotze and A.W. Thomson, editors. Academic Press, London. 373–384.

Shi, F.D., and L. Van Kaer. 2006. Reciprocal regulation between natural killer cells and autoreactive T cells. *Nat. Rev. Immunol.* 6:751–760. doi:10.1038/nri1935

Shi, F.D., H.B. Wang, H. Li, S. Hong, M. Taniguchi, H. Link, L. Van Kaer, and H.G. Ljunggren. 2000. Natural killer cells determine the outcome of B cell-mediated autoimmunity. *Nat. Immunol.* 1:245–251. doi:10.1038/79792

Steinman, L. 1996. Multiple sclerosis: a coordinated immunological attack against myelin in the central nervous system. *Cell*. 85:299–302. doi:10.1016/S0092-8674(00)81107-1

Tomasec, P., V.M. Braud, C. Rickards, M.B. Powell, B.P. McSharry, S. Gadola, V. Cerundolo, L.K. Borysiewicz, A.J. McMichael, and G.W. Wilkinson. 2000. Surface expression of HLA-E, an inhibitor of natural killer cells, enhanced by human cytomegalovirus gpUL40. *Science*. 287:1031. doi:10.1126/science.287.5455.1031

Tracey, K.J. 2009. Reflex control of immunity. *Nat. Rev. Immunol.* 9:418–428. doi:10.1038/nri2566

Vandenbark, A.A., J. Huan, M. Agotsch, D. La Tocha, S. Goelz, H. Offner, S. Lanker, and D. Bourdette. 2009. Interferon-beta-1a treatment increases CD56bright natural killer cells and CD4+CD25+ Foxp3 expression in subjects with multiple sclerosis. *J. Neuroimmunol.* 215:125–128. doi:10.1016/j.jneuroim.2009.08.007

Weber, M.S., T. Prod'homme, S. Youssef, S.E. Dunn, C.D. Rundle, L. Lee, J.C. Patarroyo, O. Stüve, R.A. Sobel, L. Steinman, and S.S. Zamvil. 2007. Type II monocytes modulate T cell-mediated central nervous system autoimmune disease. *Nat. Med.* 13:935–943. doi:10.1038/nm1620

Weiner, H.L., and D.J. Selkoe. 2002. Inflammation and therapeutic vaccination in CNS diseases. *Nature*. 420:879–884. doi:10.1038/nature01325

Wekerle, H. 1998. The viral triggering of autoimmune disease. *Nat. Med.* 4:770–771. doi:10.1038/nm0798-770

Wu, H.J., H. Sawaya, B. Binstadt, M. Brickelmaier, A. Blasius, L. Gorelik, U. Mahmood, R. Weissleder, J. Carulli, C. Benoist, and D. Mathis. 2007. Inflammatory arthritis can be reined in by CpG-induced DC–NK cell cross talk. *J. Exp. Med.* 204:1911–1922. doi:10.1084/jem.20070285

Wynn, D., M. Kaufman, X. Montalban, T. Vollmer, J. Simon, J. Elkins, G. O'Neill, L. Neyer, J. Sheridan, C. Wang, et al; CHOICE investigators. 2010. Daclizumab in active relapsing multiple sclerosis (CHOICE study): a phase 2, randomised, double-blind, placebo-controlled, add-on trial with interferon beta. *Lancet Neurol.* 9:381–390. doi:10.1016/S1474-4422(10)70033-8

Xu, W., G. Fazekas, H. Hara, and T. Tabira. 2005. Mechanism of natural killer (NK) cell regulatory role in experimental autoimmune encephalomyelitis. *J. Neuroimmunol.* 163:24–30. doi:10.1016/j.jneuroim.2005.02.011

Yang, L., D.E. Anderson, C. Baecher-Allan, W.D. Hastings, E. Bettelli, M. Oukka, V.K. Kuchroo, and D.A. Hafler. 2008. IL-21 and TGF-beta are required for differentiation of human T(H)17 cells. *Nature*. 454:350–352. doi:10.1038/nature07021

Yokoyama, W.M., and B.F. Plougastel. 2003. Immune functions encoded by the natural killer gene complex. *Nat. Rev. Immunol.* 3:304–316. doi:10.1038/nri1055

Zhang, B., T. Yamamura, T. Kondo, M. Fujiwara, and T. Tabira. 1997. Regulation of experimental autoimmune encephalomyelitis by natural killer (NK) cells. *J. Exp. Med.* 186:1677–1687. doi:10.1084/jem.186.10.1677

Zhou, L., M.M. Chong, and D.R. Littman. 2009. Plasticity of CD4+ T cell lineage differentiation. *Immunity*. 30:646–655. doi:10.1016/j.immuni.2009.05.001